



## Fertilization by coral-dwelling fish promotes coral growth but can exacerbate bleaching response

A. Raine Detmer <sup>a,\*</sup>, Ross Cunning <sup>b</sup>, Ferdinand Pfab <sup>a</sup>, Alexandra L. Brown <sup>a</sup>, Adrian C. Stier <sup>a</sup>, Roger M. Nisbet <sup>a</sup>, Holly V. Moeller <sup>a</sup>

<sup>a</sup> Department of Ecology, Evolution, and Marine Biology, University of California, Santa Barbara, Santa Barbara, CA 93106, USA

<sup>b</sup> Daniel P. Haerther Center for Conservation and Research, John G. Shedd Aquarium Chicago, IL 60605, USA

### ARTICLE INFO

#### Article history:

Received 23 November 2021

Revised 28 February 2022

Accepted 2 March 2022

Available online 8 March 2022

#### Keywords:

DEB modeling

Coral bleaching

Fish excretions

Nitrogen fertilization

Symbiosis

Coral-associated fauna

### ABSTRACT

Many corals form close associations with a diverse assortment of coral-dwelling fishes and other fauna. As coral reefs around the world are increasingly threatened by mass bleaching events, it is important to understand how these biotic interactions influence corals' susceptibility to bleaching. We used dynamic energy budget modeling to explore how nitrogen excreted by coral-dwelling fish affects the physiological performance of host corals. In our model, fish presence influenced the functioning of the coral-Symbiodiniaceae symbiosis by altering nitrogen availability, and the magnitude and sign of these effects depended on environmental conditions. Although our model predicted that fish-derived nitrogen can promote coral growth, the relationship between fish presence and coral tolerance of photo-oxidative stress was non-linear. Fish excretions supported denser symbiont populations that provided protection from incident light through self-shading. However, these symbionts also used more of their photosynthetic products for their own growth, rather than sharing with the coral host, putting the coral holobiont at a higher risk of becoming carbon-limited and bleaching. The balance between the benefits of increased symbiont shading and costs of reduced carbon sharing depended on environmental conditions. Thus, while there were some scenarios under which fish presence increased corals' tolerance of light stress, fish could also exacerbate bleaching and slow or prevent subsequent recovery. We discuss how the contrast between the potentially harmful effects of fish predicted by our model and results of empirical studies may relate to key model assumptions that warrant further investigation. Overall, this study provides a foundation for future work on how coral-associated fauna influence the bioenergetics of their host corals, which in turn has implications for how these corals respond to bleaching-inducing stressors.

© 2022 The Authors. Published by Elsevier Ltd. This is an open access article under the CC BY-NC-ND license (<http://creativecommons.org/licenses/by-nc-nd/4.0/>).

### 1. Introduction

Coral reefs are among the most productive and biodiverse ecosystems on the planet (Crossland et al., 1991; Fisher et al., 2015). This diversity is largely supported by the physical structure of the reefs themselves, which is primarily composed of the calcium carbonate skeletons of scleractinian corals (Graham and Nash, 2013; Spalding et al., 2001). Coral reefs generally occur in nutrient-poor waters, yet corals are able to calcify at a rate that supports net reef accretion due to a symbiosis with endosymbiotic algae in the family Symbiodiniaceae (Muscatine and Porter, 1977). In this partnership, the coral provides its algae with nutrients and carbon dioxide needed for photosynthesis, and the algae provide fixed carbon that fuels coral growth (Davy et al., 2012).

The functioning of the coral-algal symbiosis is critical for the persistence of coral reef ecosystems. However, thermal and other stressors can cause this relationship to break down, leading to the mass expulsion of symbionts known as coral bleaching (Hoegh-Guldberg, 1999). Severe bleaching events can result in coral mortality, and they are currently the primary threat to coral reefs worldwide (Hughes et al., 2018; Eakin et al., 2019). Bleaching commonly occurs when elevated temperatures lead to photo-oxidative stress in the symbionts, triggering their expulsion by the host coral. However, many factors influence whether and to what degree an individual coral bleaches during a stress event, including symbiont type, nutrient availability, level of heterotrophic feeding, host morphology, and history of stress exposure (Rowan, 2004; Morris et al., 2019; Grottoli et al., 2006; Loya et al., 2001; Hackerott et al., 2021). As stress events like marine heatwaves increase in frequency and severity (Hughes et al., 2018), there is a critical need to better understand what makes

\* Corresponding author.

E-mail address: [adetmer@ucsb.edu](mailto:adetmer@ucsb.edu) (A.R. Detmer).

corals more or less susceptible to bleaching. However, in many cases, this is challenging because the factors that modulate bleaching susceptibility do so in complex ways. For example, although high ambient concentrations of nutrients have been shown to exacerbate bleaching (Thurber et al., 2014; Donovan et al., 2020), the effects of nutrient enrichment on bleaching depend on numerous factors (e.g., the form of nitrogen, N:P ratios) in ways that are not fully understood (Morris et al., 2019; Wiedenmann et al., 2013). Additionally, coral growth has been shown to exhibit a unimodal response to nutrient enrichment (Gil, 2013), which could potentially extend to similarly non-linear effects of nutrients on bleaching.

Corals' tolerance of bleaching-inducing stressors may also be influenced by other organisms. In addition to algal endosymbionts, a diverse assortment of taxa may live on or within coral colonies (Gates and Ainsworth, 2011). In particular, the structural complexity created by branching corals in the genera *Pocillopora* and *Acropora* serves as an important habitat for many species of fishes and invertebrates (Coker et al., 2014; Stella et al., 2010). Host corals receive a range of benefits from these inhabitants, including enhanced defense against corallivores, removal of sediments, and provision of nutrients (McKeon et al., 2012; Stewart et al., 2006; Liberman et al., 1995). The presence of coral-associated fauna may also ameliorate the effects of stressors like disease and elevated temperatures (Pollock et al., 2013; Chase et al., 2018), suggesting that these mutualistic relationships could significantly influence the bleaching susceptibility of the corals that form them (Gates and Ainsworth, 2011).

Coral-dwelling fishes, particularly damselfish (Family Pomacentridae), are widespread and abundant on many coral reefs (Coker et al., 2014; Wilson et al., 2008). How these fish impact their host colonies during periods of stress could therefore have large implications for the resilience of branching coral populations. However, little is known about how fish presence influences coral bleaching, or by what mechanisms. One recent study found that resident fish reduced the severity of experimentally-induced bleaching, and the authors suggested these results could be due to increased nutrient availability and/or aeration of interstitial space in the presence of fish (Chase et al., 2018). Here, we explored this hypothesis more formally and expanded on it by also asking how fish effects are mediated by environmental conditions, including ambient nitrogen levels. We focused on the effects of fish excretions (e.g., nitrogenous wastes; Meyer and Schultz, 1985), as nutrient availability can have a major influence on corals' susceptibility to bleaching (Morris et al., 2019). In general, fishes and other consumers play important roles in nutrient dynamics on coral reefs, including the transport of nutrients from the water column to the benthos (Allgeier et al., 2016; Pinnegar and Polunin, 2006). Coral-dwelling fishes may have particularly large impacts on the availability of nutrients for individual coral colonies, as they are often site-attached (Booth, 2016) and inhabit colony interstices, where nutrient levels may differ from those of the surrounding water column due to colony uptake rates and flow patterns (Chamberlain and Graus, 1975). While the nutrients excreted by coral-dwelling fish have been shown to increase the growth rates of their host corals under ambient conditions (Holbrook et al., 2008), our goal with this study was to investigate how these excretions then modulate the host's response to stressors capable of triggering bleaching.

A mechanistic understanding of the effects of fish-derived nitrogen on host corals requires explicit consideration of the bioenergetics of the coral-algal symbiosis. Dynamic energy budget (DEB) models, which essentially model an organism's physiology by tracking the fluxes of elements within it (Kooijman, 2009), provide a theoretical framework to explore the effects of fish excretions. Here, we modified a DEB-based model of the coral-algal symbiosis

(Cunning et al., 2017) to include nutrient excretion by coral-dwelling fish. Our goal was to investigate how fish excretions may affect host corals during periods of low and elevated stress, as well as the environmental factors that mediate these effects. We first used the model to explore how fish affected nitrogen availability and host growth under various ambient (low stress) environmental conditions. We then simulated acute stress events to investigate the sensitivity of host bleaching to nitrogen availability and the underlying mechanisms. Finally, we looked at effects of fish excretion on host bleaching thresholds and post-bleaching recovery dynamics and how these depended on environmental conditions. This study is an important step towards a more mechanistic understanding of how coral-dwelling fishes may influence the growth and stress tolerance of host corals on reefs that are increasingly impacted by the effects of global climate change.

## 2. Model description

Our model is based on a dynamic bioenergetic model of the coral-algal symbiosis built by Cunning et al. (2017). In this section, we provide a brief overview of this model before describing how we modified it to incorporate nitrogen excretion by coral-dwelling fish. A detailed description of the original model and its equations is given in Appendix A.

### 2.1. The coral-algal DEB model

The Cunning et al. model describes the bioenergetics of the symbiosis between a coral host and its algal symbionts. It consists of two state variables (host and symbiont biomass) and 14 mass-specific fluxes that describe the flows of nitrogen, carbon and light energy within the system, as well as the formation and turnover of host and symbiont biomass (Table 1, "Host" and "Symbiont" boxes in Fig. 1). Equations describing the production of fixed carbon and biomass from substrates are referred to as synthesizing units (SUs). The symbiosis is characterized by "sharing the surplus", whereby each partner provides the other with substrate (nitrogen from the host and fixed carbon from the symbiont) in excess of that used for its own growth.

Within the symbiont, a photosynthesis SU takes in light and CO<sub>2</sub> and produces fixed carbon. This fixed carbon, together with surplus nitrogen received from the host, is used by the symbiont biomass SU to make symbiont biomass. The host takes up nitrogen and prey (which consists of nitrogen and carbon) from the environment. This nitrogen and carbon, along with surplus fixed carbon from the symbiont, is input into the host biomass SU and used to produce host biomass. Additionally, organic carbon in excess of that used for host growth fuels host carbon concentrating mechanisms (CCMs), which supply the symbiont with CO<sub>2</sub>.

The symbiosis is functional when the production and supply of fixed carbon is high enough that it is not limiting the growth of either partner. Symbiont and host growth rates are both positive and limited by the availability of nitrogen (or, if nitrogen levels are high, by maximum biomass production rates). We refer to this non-bleached, "healthy" state as the "nitrogen-limited state" throughout the paper. Host bleaching is characterized by a flip to a carbon-limited state in which the production of fixed carbon and assimilation of carbon from prey are insufficient to support positive growth of the host and symbiont (Wooldridge, 2009). Bleaching is triggered by excess light energy, which produces reactive oxygen species (ROS). These molecules inhibit photosynthesis and increase symbiont turnover, reducing the production of fixed carbon and potentially causing the system to become carbon limited.

**Table 1**

Model fluxes, adapted from [Cunning et al. \(2017\)](#). Fluxes that were modified from the original model are in bold.

Symbol	Description	Units	Eq. No.
$j_N$	<b>Total nitrogen uptake rate</b>	mol N C-mol H <sup>-1</sup> d <sup>-1</sup>	4
$j_{N_{env}}$	<b>Environmental (ambient) nitrogen uptake rate</b>	mol N C-mol H <sup>-1</sup> d <sup>-1</sup>	4
$j_{N_i}$	<b>Interstitial nitrogen uptake rate</b>	mol N C-mol H <sup>-1</sup> d <sup>-1</sup>	4
$j_{NW}$	Waste nitrogen from symbiont	mol N C-mol S <sup>-1</sup> d <sup>-1</sup>	6
$j_X$	Prey assimilation (feeding) rate	C-mol X C-mol H <sup>-1</sup> d <sup>-1</sup>	A4
$j_{HT}$	Host biomass turnover rate	C-mol H C-mol H <sup>-1</sup> d <sup>-1</sup>	A5
$r_{NH}$	Recycled nitrogen from host turnover	mol N C-mol H <sup>-1</sup> d <sup>-1</sup>	A6
$j_{HG}$	Host biomass formation rate	C-mol H C-mol H <sup>-1</sup> d <sup>-1</sup>	A7
$\rho_N$	Nitrogen shared with the symbiont	mol N C-mol H <sup>-1</sup> d <sup>-1</sup>	A8
$j_{eC}$	Excess carbon used to activate host CCMs	mol C C-mol H <sup>-1</sup> d <sup>-1</sup>	A9
$j_{CO_2}$	CO <sub>2</sub> input to photosynthesis	mol CO <sub>2</sub> C-mol H <sup>-1</sup> d <sup>-1</sup>	A10
$j_L$	Light absorption rate	mol photons C-mol S <sup>-1</sup> d <sup>-1</sup>	A11
$r_{CH}$	Recycled CO <sub>2</sub> from host	mol CO <sub>2</sub> C-mol H <sup>-1</sup> d <sup>-1</sup>	A13
$r_{CS}$	Recycled CO <sub>2</sub> from symbiont	mol CO <sub>2</sub> C-mol S <sup>-1</sup> d <sup>-1</sup>	A14
$j_{CP}$	Photosynthesis rate	mol C C-mol S <sup>-1</sup> d <sup>-1</sup>	A15
$j_{el}$	Light energy in excess of photochemistry	mol photons C-mol S <sup>-1</sup> d <sup>-1</sup>	A16
$j_{NPQ}$	Total capacity of NPQ	mol photons C-mol S <sup>-1</sup> d <sup>-1</sup>	A17
$c_{ROS}$	ROS production proportional to baseline	–	A18
$j_{ST}$	Symbiont biomass turnover rate	C-mol S C-mol S <sup>-1</sup> d <sup>-1</sup>	A19
$r_{NS}$	Recycled nitrogen from symbiont turnover	mol N C-mol S <sup>-1</sup> d <sup>-1</sup>	A20
$j_{SG}$	Symbiont biomass formation rate	C-mol S C-mol S <sup>-1</sup> d <sup>-1</sup>	A21
$\rho_C$	Fixed carbon shared with host	mol C C-mol S <sup>-1</sup> d <sup>-1</sup>	A22

In the [Cunning et al. \(2017\)](#) model, the host takes up nitrogen from the external environment, which is assumed to be the surrounding water column. To understand how the presence of fish affects the amount of nitrogen available to the host, we chose to explicitly account for the dynamics of the concentration of nitrogen within the interstitial space of a coral colony. These modifications are described below (also see [Fig. 1](#)).

## 2.2. Host colony morphology

In the dynamic energy budget model, the host is described in terms of tissue biomass. In order to characterize the morphology of a host colony, we distinguished between living tissue (the host biomass) and skeleton volume (which determines the volume of the interstitial space). We used empirical data on branching corals to approximate simple allometric relationships between host tissue biomass  $H$  and metrics of colony morphology (see “*Fish excretion model parameterization*” supplement). For total colony volume  $V_H$ , we used the general relationship

$$V_H = k_V H \quad (1)$$

where  $k_V$  is colony volume per unit biomass (see [Table 2](#) for a description of model variables, parameters, and their units). Thus, the DEB-based component of the model describes the biomass of

living host tissue, and we assume that when new tissue biomass is formed, the coral simultaneously builds skeleton and  $V_H$  increases at a rate proportional to  $dH/dt$ . However, since it is mainly the skeletal structure of a colony that determines its volume, the above relationship no longer holds when a host loses tissue biomass but its skeleton remains intact (such as may occur following bleaching; [Clark et al., 2000](#)). To address this, the rate of change in host volume was decoupled from that of host biomass:

$$\frac{dV_H}{dt} = \begin{cases} 0, & \frac{dH}{dt} < 0 \\ k_V \frac{dH}{dt}, & \frac{dH}{dt} \geq 0 \end{cases} \quad (2)$$

When host tissue biomass is declining,  $V_H$  remains constant. When host biomass is increasing,  $V_H$  increases proportionately to  $dH/dt$  as given by the derivative of eqn. 1 with respect to time. Note this formulation assumes that, following a period of negative host growth (e.g., a bleaching event), a host that returns to positive growth will begin growing new tissue and new skeleton. In reality, re-growth of tissue over old skeleton may also occur ([Henry and Hart, 2005](#)), but for simplicity was not considered here.

The volume of the interstitial space in a colony  $V_{Hi}$  is then given by

$$V_{Hi} = \nu_i V_H \quad (3)$$

where  $\nu_i$  is the fraction of the colony volume that is filled with water.

## 2.3. Host nitrogen uptake

As in the [Cunning et al. \(2017\)](#) model, the rate of nitrogen uptake by the host is described by Michaelis-Menten kinetics. However, there are now two pools of nitrogen available to the host: nitrogen in the external environment  $N_{env}$  (equivalent to  $N$  in the original model) and nitrogen in the interstitial space  $N_i$ . We assumed that a fraction  $\alpha$  of host tissue is in direct contact with the external environment and exclusively takes up environmental nitrogen. The remaining  $(1 - \alpha)$  fraction of host tissue lines the interstitial space and only has access to interstitial nitrogen. Assuming the same maximum uptake rate  $j_{Nm}$  and half-saturation constant  $K_N$  for both nitrogen pools, the total mass-specific (per unit host biomass) rate of nitrogen uptake  $j_N$  is therefore given by

$$j_N = \alpha j_{N_{env}} + (1 - \alpha) j_{N_i} = \alpha \frac{j_{Nm} N_{env}}{N_{env} + K_N} + (1 - \alpha) \frac{j_{Nm} N_i}{N_i + K_N} \quad (4)$$

## 2.4. Fish growth

Fish  $P$  grow logistically at an intrinsic growth rate  $r_p$  to a carrying capacity that scales with the constant  $k_p$  to the amount of living host tissue in the interstitial space,  $(1 - \alpha)H$ :

$$\frac{dP}{Pdt} = r_p \left( \frac{k_p (1 - \alpha) H - P}{k_p (1 - \alpha) H} \right) \quad (5)$$

We assume that fish carrying capacity is mainly determined by interstitial space, as studies suggest competition for shelter space underlies density-dependence in coral-dwelling damselfishes ([Holbrook and Schmitt, 2002](#)). The decision to scale fish carrying capacity to the biomass of interstitial tissue (rather than interstitial volume) implies that a bleached coral that has experienced tissue mortality will not support as many fish as an undamaged coral with an equivalent interstitial volume. This formulation was based on the assumption that coral-dwelling fish prefer live coral as hosts ([Wilson et al., 2008; Coker et al., 2014](#)) and will therefore leave dying hosts in the weeks following the onset of bleaching. However, we also explored how making fish carrying capacity a func-

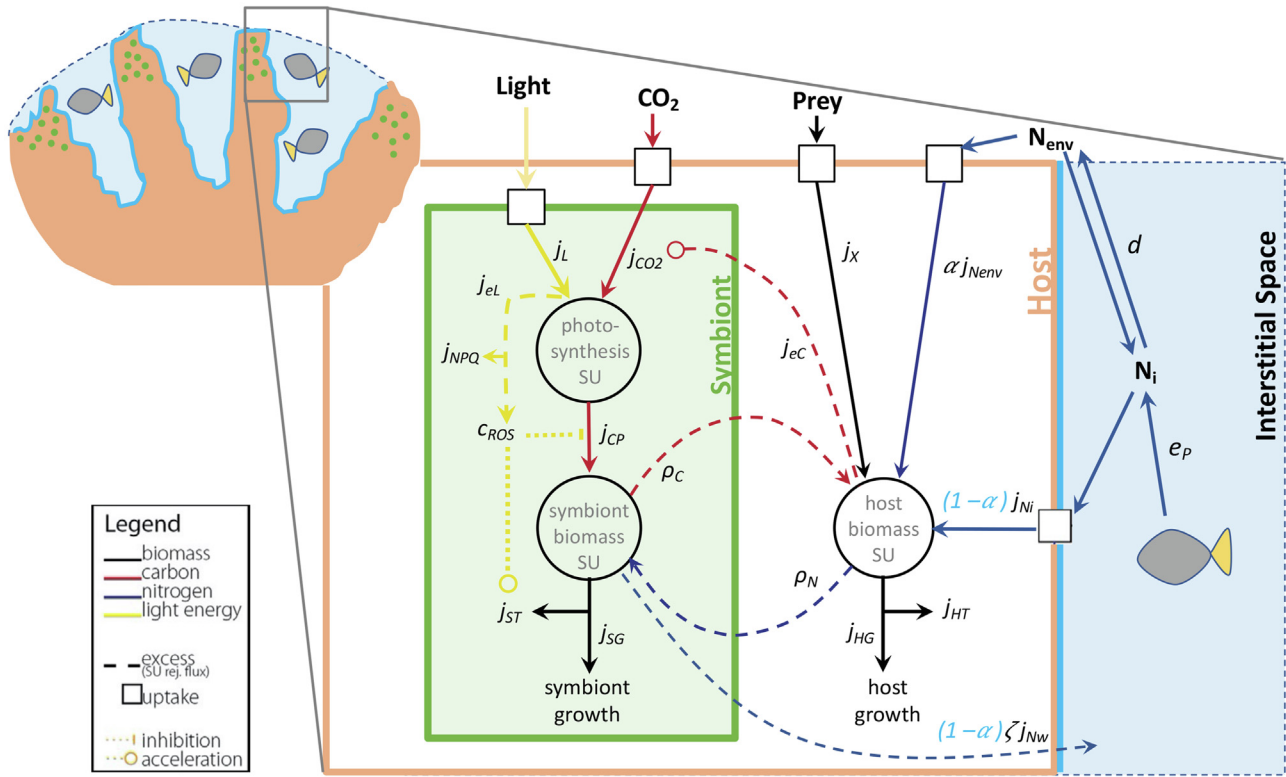


**Fig. 1.** Conceptual diagram of the model (modified from Fig. 1 of Cunning et al., 2017). As in Cunning et al.,  $j$ 's represent mass-specific fluxes, and large circles represent synthesizing units (SUs).  $\rho$ 's signify fluxes that are shared between partners. In the fish excretion model, the host takes up nitrogen from both the external environment ( $N_{env}$ ) and the interstitial space ( $N_i$ ) at rates proportional to the fraction of host tissue in contact with each of these environments ( $\alpha$  and  $1 - \alpha$ , respectively). The concentration of nitrogen in the interstitial space is influenced by uptake by the host, exchange with the external environment, waste released by the symbionts, and excretions from fish within the interstitial space.

tion of interstitial volume (meaning that fish remain on bleached hosts; Coker et al., 2012) altered their effects on post-bleaching dynamics.

## 2.5. Interstitial nitrogen dynamics

The concentration of nitrogen in the interstitial space  $N_i$  is a state variable whose dynamics are influenced by 1) exchange of water (and dissolved nitrogen) between the interstitial space and external environment, 2) excretions from fish, 3) waste nitrogen released by the symbiont, and 4) uptake by the host. Note that many forms of nitrogen including nitrate, ammonium, and urea may be found on coral reefs, and their origins and effects on the coral holobiont may vary (Shantz and Burkepile, 2014). However, for the purposes of our present work, we adopt the simplifying assumption that all nitrogen available to the coral is of the same chemical form, which allows us to focus our analysis on the effects of absolute changes in nitrogen supply. We consider the probable consequences of alternate formulations in the Discussion.

1) We assumed that the rate of nitrogen exchange between the interstitial space and external environment depends on the difference between interstitial and ambient nitrogen concentrations and a flushing rate  $d$ :

$$d(N_{env} - N_i)$$

where  $d$  represents the rate of turnover of the water in the interstitial space. Its value may be influenced by colony morphology (e.g., colonies with more open branching structures would be expected to have higher flushing rates) as well as the rate of water flow around a colony (Reidenbach et al., 2006).

2) Fish excrete nitrogen into the interstitial space at a per biomass rate  $e_p$ . The total rate of nitrogen excretion is assumed to

scale linearly with fish biomass (Holbrook et al., 2008), and is thus given by  $e_p P$ .

3) Recall that the host shares nitrogen in excess of that used for its own growth with the symbiont. Any nitrogen that is still left over after the symbiont has used all it can for growth makes up a rejection flux of nitrogen from the symbiont biomass SU,  $j_{Nw}$ . This flux is the difference between the input of nitrogen to the SU (i.e., surplus nitrogen from the host,  $\rho_N H/S$ , and recycled nitrogen from symbiont turnover,  $r_{NS}$ ) and the amount of nitrogen used for symbiont biomass formation,  $\eta_{NS} j_{SG}$ :

$$j_{Nw} = \left( \rho_N \frac{H}{S} + r_{NS} - \eta_{NS} j_{SG} \right)_+ \quad (6)$$

Note that  $x()_+$  means  $\max(x, 0)$  and ensures that  $j_{Nw}$  never goes negative. In the original Cunning et al. (2017) model, this waste nitrogen was assumed to be lost to the environment. Here, in the absence of empirical data on the fate of this nitrogen, we assumed that waste nitrogen released by the symbionts in host tissue lining the interstitial space can enter this space. We further assumed that a fraction  $\zeta$  of this nitrogen is in a form that is bioavailable to the host. If symbionts are evenly distributed in host tissue, such that a fraction  $(1 - \alpha)$  of symbionts are within tissue lining the interstitial space, then the total amount of waste nitrogen that enters the interstitial space and is available to the host is

$$\zeta(1 - \alpha) j_{Nw} S$$

4) As described in the section "Host nitrogen uptake", the mass-specific rate of nitrogen uptake from the interstitial space by the host is  $(1 - \alpha) j_{N_i}$  (eqn. 4). Thus, the total rate of host interstitial nitrogen uptake is given by

$$(1 - \alpha) j_{N_i} H$$

**Table 2**

Model state variables and parameters, adapted from [Cunning et al. \(2017\)](#). Additions to the original model are shown in bold. Details on model parameterization are provided in the supplement. For parameters whose values were varied in simulations, the default values are given.

Symbol	Description	Units	Value
<b>State variables</b>			
<i>H</i>	Host tissue biomass	C-mol	–
<i>S</i>	Symbiont biomass	C-mol	–
<b>P</b>	<b>Fish biomass</b>	g	–
<b>V<sub>H</sub></b>	<b>Volume of host colony</b>	L	–
<b>V<sub>Hi</sub></b>	<b>Volume of the interstitial space of host colony</b>	L	–
<b>N<sub>i</sub></b>	<b>Concentration of nitrogen in the interstitial space</b>	mol L <sup>-1</sup>	–
<i>t</i>	Time	d	–
<b>Parameters</b>			
<i>N<sub>env</sub></i>	Concentration of nitrogen in the external environment	mol L <sup>-1</sup>	1*10 <sup>-7</sup>
<i>X</i>	Concentration of prey	C-mol X L <sup>-1</sup>	1*10 <sup>-7</sup>
<i>I</i>	Ambient irradiance	mol photons m <sup>-2</sup> d <sup>-1</sup>	15
<b>k<sub>V</sub></b>	<b>Host colony volume per unit biomass</b>	L C-mol H <sup>-1</sup>	16.9
<b>v<sub>i</sub></b>	<b>Fraction of host colony volume that is interstitial space</b>	–	0.7
$\alpha$	<b>Fraction of host tissue in contact with external environment</b>	–	0.23
<i>r<sub>p</sub></i>	Fish growth rate	d <sup>-1</sup>	0.05
<b>k<sub>P</sub></b>	<b>Scalar relating fish carrying capacity to interstitial host tissue biomass</b>	g fish C-mol H <sup>-1</sup>	210
<i>d</i>	Flushing rate	d <sup>-1</sup>	1660
$\zeta$	<b>Fraction of symbiont waste N bioavailable to host</b>	–	1
<i>e<sub>P</sub></i>	Fish excretion rate	mol N g fish <sup>-1</sup> d <sup>-1</sup>	1.5*10 <sup>-5</sup>
<i>n<sub>NH</sub></i>	N:C molar ratio in host biomass	–	0.18
<i>n<sub>NS</sub></i>	N:C molar ratio in symbiont biomass	–	0.13
<i>n<sub>NX</sub></i>	N:C molar ratio in prey biomass	–	0.2
<i>j<sub>HT</sub><sup>0</sup></i>	Maintenance rate of host biomass	C-mol H C-mol H <sup>-1</sup> d <sup>-1</sup>	0.03
<i>j<sub>ST</sub><sup>0</sup></i>	Maintenance rate of symbiont biomass	C-mol S C-mol S <sup>-1</sup> d <sup>-1</sup>	0.03
$\sigma_{NH}$	Proportion N turnover recycled in host	–	0.9
$\sigma_{CH}$	Proportion host metabolic CO <sub>2</sub> recycled to photosynthesis	–	0.1
$\sigma_{NS}$	Proportion N turnover recycled in symbiont	–	0.9
$\sigma_{CS}$	Proportion symbiont metabolic CO <sub>2</sub> recycled to photosynthesis	–	0.9
<i>j<sub>Xm</sub></i>	Maximum prey assimilation rate from host feeding	C-mol X C-mol H <sup>-1</sup> d <sup>-1</sup>	0.13
<i>K<sub>X</sub></i>	Half-saturation constant for prey assimilation	C-mol X L <sup>-1</sup>	10 <sup>-6</sup>
<i>j<sub>Nm</sub></i>	Maximum host DIN uptake rate	mol N C-mol H <sup>-1</sup> d <sup>-1</sup>	0.035
<i>K<sub>N</sub></i>	Half-saturation constant for host DIN uptake	mol N L <sup>-1</sup>	1.5 · 10 <sup>-6</sup>
<i>k<sub>CO<sub>2</sub></sub></i>	Efficacy of CO <sub>2</sub> delivery to photosynthesis by host CCMs	mol CO <sub>2</sub> mol C <sup>-1</sup>	10
<i>j<sub>HGm</sub></i>	Maximum specific growth rate of host	C-mol H C-mol H <sup>-1</sup> d <sup>-1</sup>	1
<i>y<sub>CL</sub></i>	Quantum yield of photosynthesis	mol C mol photons <sup>-1</sup>	0.1
<i>y<sub>C</sub></i>	Yield of biomass formation from carbon	C-mol mol C <sup>-1</sup>	0.8
$\bar{a}^*$	Effective light-absorbing cross-section of symbiont	m <sup>2</sup> C-mol S <sup>-1</sup>	1.34
<i>k<sub>NPQ</sub></i>	NPQ capacity of symbiont	mol photons C-mol S <sup>-1</sup> d <sup>-1</sup>	112
<i>k<sub>ROS</sub></i>	Excess photon energy that doubles ROS production, relative to baseline levels	mol photons C-mol S <sup>-1</sup> d <sup>-1</sup>	80
<i>j<sub>CPm</sub></i>	Maximum specific photosynthesis rate of symbiont	mol C C-mol S <sup>-1</sup> d <sup>-1</sup>	2.8
<i>j<sub>SGm</sub></i>	Maximum specific growth rate of symbiont	C-mol S C-mol S <sup>-1</sup> d <sup>-1</sup>	0.25
<i>b</i>	Scaling parameter for bleaching response	–	5

Putting the above components together, the full equation for the interstitial nitrogen dynamics is

$$\frac{dN_i}{dt} = d(N_{env} - N_i) + (e_P P + \zeta(1 - \alpha)j_{Nw}S - (1 - \alpha)j_{N_i}H) V_{Hi}^{-1} \quad (7)$$

where components 2–4 are divided by the volume of the interstitial space  $V_{Hi}$  to express these rates of nitrogen transfer in terms of nitrogen concentrations.

## 2.6. Model initialization

In this model, the dynamics of the fluxes occur on faster time scales than the dynamics of the state variables. While the fluxes are assumed to equilibrate virtually immediately, the flux equations can be satisfied by multiple sets of solutions. To simulate the system, we set up auxiliary state variables for some of the fluxes ( $\rho_c$ ,  $j_{CP}$  and  $j_{N_i}$ ) and calculated the equilibria of the remaining fluxes from these. The numerical method and the procedure for finding a low dimensional representation of the fast network are described by [Pfab et al. \(in review\)](#). Using this method, the system can be fully defined by specifying initial values for  $\rho_c$ ,  $j_{CP}$ , and  $j_{N_i}$  in addition to the state variables  $H$ ,  $V_H$ ,  $S$ ,  $N_i$ , and  $P$ . In all simulations, the initial values used were  $H_0 = 1$ ,  $V_{H0} = k_V H_0$ ,

$S_0 = 0.3$ ,  $N_{i0} = N_{env}$ ,  $j_{N_i0} = \frac{j_{Nm}N_{i0}}{N_{i0} + K_N}$ ,  $j_{CP0} = 1$ , and  $\rho_{CO} = 1$ . If fish were present, fish biomass was initialized at carrying capacity ( $P_0 = k_P(1 - \alpha)H_0$ ), otherwise  $P_0 = 0$ . For a given set of environmental conditions, the steady state behavior of the system is determined by the initial values of a few key fluxes ([Pfab et al., in review](#)). By choosing  $j_{CP0} = 1$  and  $\rho_{CO} = 1$ , we ensured that the system was initially in the nitrogen-limited (non-bleached) state: the symbiont is both producing carbon and sharing it with the host at a high rate.

## 3. Model analysis and results

### 3.1. Fish effects on interstitial nitrogen and host growth under varying environmental conditions

#### 3.1.1. Description of analyses

To explore the conditions under which fish-derived nitrogen benefits host corals, we first focused on constant environments with intermediate light levels ( $I = 15$  mol photons m<sup>-2</sup> d<sup>-1</sup>). We ran simulations with varying levels of host prey ( $X$ ), ambient levels of nitrogen in the environment ( $N_{env}$ ), flushing rates ( $d$ ), and relationships between host biomass and fish carrying capacity ( $k_P$ ), all with and without fish. For each simulation, we recorded the

steady state concentration of interstitial nitrogen  $N_i$  and mass-specific host growth rate  $dH/Hdt$ . We considered the system to have reached a steady state when interstitial nitrogen and specific growth rates changed by less than 0.01% over the last 50 days of the simulation.

We estimated reasonable ranges for each of the varied parameters from empirical data. Nitrogen concentrations on coral reefs can vary widely, with nitrate and ammonium levels typically ranging from 0.05–5  $\mu\text{M}$  (O'Neil and Capone, 2008). Since we expect fish excretions to have the largest effects on corals in low nitrogen environments, we chose a range for  $N_{env}$  of 0.01–1  $\mu\text{M}$ , which is at the lower end of reported values. Like nitrogen, zooplankton concentrations on coral reefs can be extremely variable (Nakajima et al., 2014). For instance, a study on the Great Barrier Reef reported zooplankton concentrations that ranged from  $<4 \times 10^{-8}$  C-mol  $\text{L}^{-1}$  on the back reef lagoon to  $2 \times 10^{-7}$  C-mol  $\text{L}^{-1}$  on the fore reef (Roman et al., 1990), although these values are at the lower end of those reported by other studies (Nakajima et al., 2014). However, in addition to zooplankton abundance, there are other factors that must be considered when estimating rates of host feeding. Corals may only consume specific taxa and sizes of zooplankton, and they may also feed on particulate organic matter and bacteria if zooplankton are not available (Palardy et al., 2006). Importantly, the degree of heterotrophy can vary widely among individual corals (Fox et al., 2018). Given these many uncertainties, we chose to vary  $X$  from 0–2  $\times 10^{-7}$  C-mol  $\text{L}^{-1}$ , but note that our estimates of rates of host heterotrophy are uncertain. Furthermore,  $X = 0$  may be unrealistic, since most corals likely have some heterotrophic feeding, but we included this case for comparison and ran simulations with and without prey.

The range of values for the flushing rate  $d$  that we used was based on dye retention trials with *Pocillopora* colonies (Holbrook et al., 2008). However, this experiment was performed in a low-flow environment, and differences in flushing rates were largely due to colony morphology. Since flow regimes can vary at different locations on a reef (Sebens et al., 2003), we expanded this range to include larger values that represent higher flow environments and thus varied  $d$  from 450 to 4050  $\text{d}^{-1}$  (but note we do not have empirical data on an upper limit). For the parameter  $k_p$ , which scales fish carrying capacity to host biomass, we estimated a baseline value of 210 g C-mol  $\text{H}^{-1}$  using survey data on damselfish abundance and host colony size collected as part of the Holbrook et al. (2008) study. Details on parameter estimation are provided in the "Fish excretion model parameterization" supplement.

### 3.1.2. Results

The degree to which fish benefit corals is determined by the magnitude by which they increase the concentration of nitrogen in the interstitial space. In intermediate light (low stress) environments, when the system is in the non-bleached state, host and symbiont growth are generally limited by nitrogen. Higher concentrations of nitrogen in the external environment increase the amount of nitrogen available to the host, both by increasing direct uptake from the environment and by increasing nitrogen in the interstitial space (Fig. 2a). Thus, host growth rate increases with increasing ambient nitrogen (Fig. 2b). Similarly, prey provides an additional source of nitrogen as well as carbon, and host growth is always higher with prey than without (Fig. 2). Note that when prey is available, host growth does not directly reflect interstitial nitrogen concentrations (Fig. 2c, d). Prey indirectly increase interstitial nitrogen levels by increasing the amount of surplus nitrogen in the system and thus the amount of waste nitrogen released by the symbiont (Fig. S1). However, when fish are present, increasing prey availability results in fish excretions being diluted due to increased host growth rates (Fig. S1; also see below), and thus

results in lower interstitial nitrogen concentrations relative to non-feeding, slower-growing hosts (Fig. 2c).

For the range of parameter values considered here, fish have either positive or neutral effects on host growth rate. Fish are more beneficial (i.e., the difference in the growth of hosts with and without fish is greater) when ambient nitrogen and prey levels are low (Fig. 2a-d, a-d, Fig. S2a). As ambient nitrogen and/or prey availability increase, host growth rate is high regardless of fish presence and the magnitude of fish benefits are diminished. Although it makes sense that hosts that have access to sufficient nitrogen from the environment and food would not be as reliant on fish, mathematically these results are due to our model formulation: the host grows exponentially, while fish grow logistically to a carrying capacity set by host biomass. As the specific growth rate of the host increases, fish start to lag behind their rapidly increasing carrying capacity. Consequently, there are less fish per unit host biomass (and per unit volume of interstitial space), and the fish's excretions are diluted. If host growth rate surpasses that of the fish, the ratio of fish to host biomass is effectively zero, and fish have no effect on the system (Fig. S3). On natural reefs, such a phenomenon could possibly occur if fish growth is limited by factors unrelated to host coral size (e.g., prey availability; Jones, 1986).

The effects of fish are also influenced by the flushing rate and, unsurprisingly, fish carrying capacity. In the absence of fish, higher flushing rates increase the concentration of nitrogen in the interstitial space, as interstitial nitrogen that is taken up by the host is more rapidly replaced with nitrogen from the external environment (Fig. 2e). When fish are present, however, higher rates of exchange with the external environment mean that fish excretions get flushed out, and the positive effects of fish on interstitial nitrogen and host growth therefore decline with increasing flushing rates (Fig. 2e, f, Fig. S2b). Finally, as the scalar  $k_p$  modulating the relationship between host biomass and fish carrying capacity increases and there are more fish per unit host biomass, there is a larger increase in interstitial nitrogen and host growth in the presence of fish (Fig. 2g, h, Fig. S2b). Variation in  $k_p$  could reflect host morphology (e.g., branch spacing, Chase et al., 2014) as well as interspecific differences in fish social behavior. For instance, schooling damselfish might have a higher carrying capacity than territorial species such as hawkfish, which are often solitary (Kane et al., 2009).

## 3.2. Non-linear effects of nitrogen on coral bleaching

### 3.2.1. Description of analyses

Our model predicted that under certain ranges of environmental conditions fish may increase the amount of nitrogen available to their host coral. While the above analyses showed that this can be beneficial in constant environments, we were also interested in how fish excretions affected host performance during acute stress events. Fish affect the host by increasing nitrogen availability; thus, to answer this question, we first explored the effects of nitrogen on the host's response to stress. Empirical studies have demonstrated that nitrogen can exacerbate bleaching (Thurber et al., 2014; Donovan et al., 2020), and theoretical work suggests this may occur due to enhanced carbon limitation of the host under conditions of elevated nitrogen (Cunning et al., 2017). Here, we wanted to better understand the mechanisms by which nitrogen impacts the symbiosis under stress, as this provides a foundation for interpreting fish effects on host bleaching dynamics.

In this model, light is used as a proxy for stress. Light was modeled as a step function in order to analyze the effects of stress magnitude and duration independently and avoid confounding effects of rates of environmental change. At time  $t = t_{StartStress}$ , light jumps from  $I$  (ambient) to  $I + I_{High}$  and remains at this value for  $t_{High}$  days

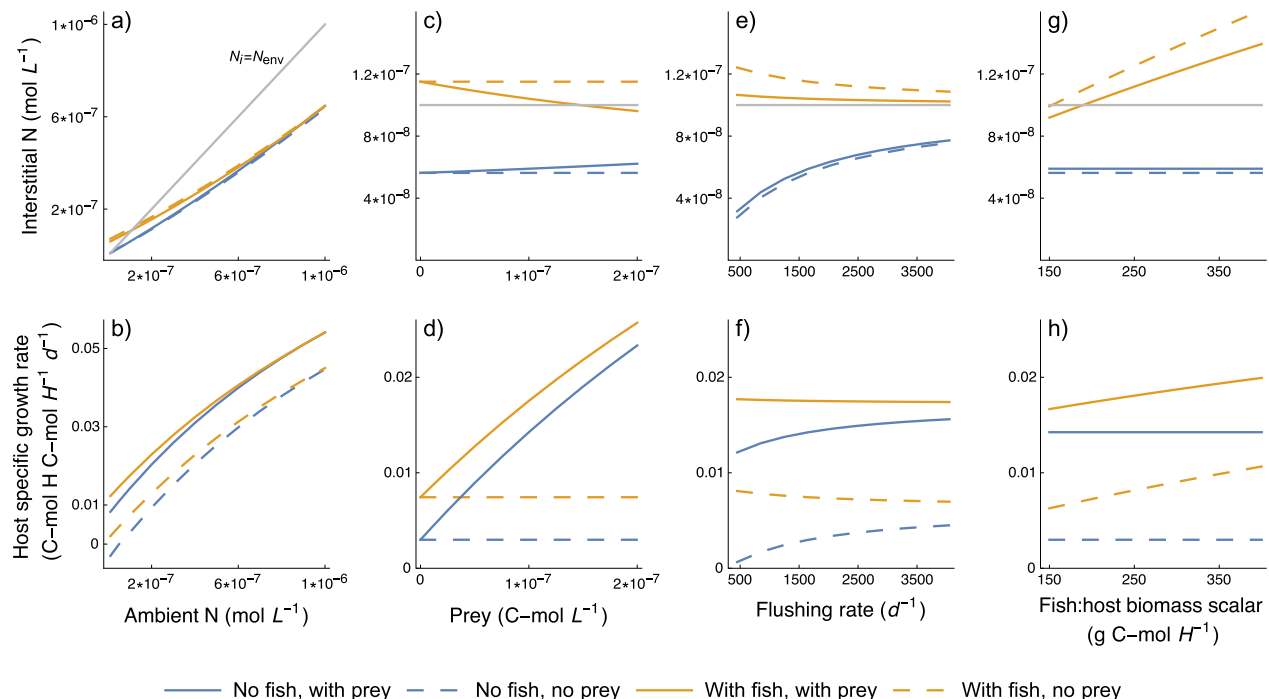


**Fig. 2.** Effects of fish and prey on steady state interstitial nitrogen concentration ( $N_i$ ) and host specific growth rate ( $dH/Hdt$ ) under varying levels of nitrogen in the external environment (a, b), levels of prey (c, d), flushing rates (e, f), and fish biomass per unit interstitial host biomass (g, h). Results are shown for simulations without fish (blue lines), with fish (orange lines), with prey (solid lines), and without prey (dashed lines). For each plot, the default values for parameters that were held constant were: flushing rate =  $1660\text{ d}^{-1}$ , scalar specifying relationship between interstitial host biomass and fish carrying capacity =  $210\text{ g C-mol H}^{-1}$ , ambient N =  $1\text{e-7 mol L}^{-1}$ , and prey =  $1\text{e-7 C-mol L}^{-1}$  (if present) or 0 C-mol L $^{-1}$  (if absent). For the interstitial nitrogen plots, the grey line indicates the ambient concentration of nitrogen in the external environment ( $N_{env}$ ). Note the difference in y-axis scales between column 1 and columns 2–4.

before dropping back to  $I$ . Although we used light pulses to simulate acute stress events, these pulses could also represent high temperature or any other stressor that disrupts the symbiont's photochemistry and drives bleaching by the production of ROS (Cunning et al., 2017).

To explore the system's sensitivity to nitrogen levels when stressed, we ran simulations in environments with low, intermediate, and high ambient concentrations of nitrogen ( $N_{env}$  = 0.1, 1, and  $10\text{ }\mu\text{M}$ , respectively). Note that the highest value used is within the range of nitrogen levels reported for reefs that are heavily impacted by anthropogenic activities (Cruz-Pinon et al., 2003). In each simulation, the system was shocked with a light pulse with a total magnitude of  $40\text{ mol photons m}^{-2}\text{ d}^{-1}$  ( $I_{High}$  =  $25\text{ mol photons m}^{-2}\text{ d}^{-1}$ ) that started on day 600 and lasted for 30 days. These simulations were run without fish or prey.

As discussed previously, bleaching occurs when the system flips to a carbon-limited state. One useful metric for determining whether the system is in this bleached state is the degree to which the production of each synthesizing unit is limited by the input of carbon (Cunning et al., 2017). Therefore, for each simulation, we calculated the relative limitations of the host and symbiont biomass SUs during and after the light pulse. This was done using eqn. 23 of Cunning et al. (2017):

$$\log\left(\frac{\min(j_{S1}, j_{Pm})}{\min(j_{S2}, j_{Pm})}\right)$$

where  $j_{S1}$  and  $j_{S2}$  are the input fluxes of carbon and nitrogen, respectively, and  $j_{Pm}$  is the maximum rate of biomass production. Positive values indicate production is more limited by nitrogen, while negative values indicate carbon is more limiting. If this expression is equal to zero, production is limited by its maximum rate (i.e., neither substrate is limiting).

### 3.2.2. Results

We found that nitrogen availability can produce a “Goldilocks effect”, in which too-low or too-high levels of nitrogen could increase the risk of host bleaching under light stress (Fig. 3, Fig. 4). Furthermore, the mechanisms underlying the effects of low vs. high nitrogen differed (Fig. 3).

In the low nitrogen environment (Fig. 3a; Fig. 4, yellow lines), hosts grew slowly prior to light stress and had little surplus nitrogen to share with the symbionts, which consequently also had a low growth rate (Fig. 4a-c). Therefore, symbiont density was initially low (Fig. 4d). Low self-shading by the sparse symbionts meant that when the light pulse occurred, symbiont photosystems were saturated, and excess light drove high levels of ROS production (Fig. 4e). These damaged the photosystems and drove declines in symbiont biomass, both of which reduced the amount of fixed carbon being produced and shared with the host (Fig. 4c, f). The host became carbon-limited and, with no surplus carbon to activate the CCMs, carbon limitation of the symbionts soon followed (Fig. 4g, h).

In the high nitrogen environment (Fig. 3b; Fig. 4, blue lines), higher host growth rate, surplus nitrogen, and symbiont growth rate meant that symbiont densities at the start of the light pulse were high (Fig. 4a-d). Because dense symbionts shaded one another, the increase in ROS production at the start of the light pulse was low (Fig. 4e). Although carbon production was reduced, symbionts were initially able to maintain positive growth (Fig. 4c). The combination of a large, growing symbiont population and lower carbon production meant that the amount of surplus carbon shared with the host declined (Fig. 4f). The host, which also required high levels of carbon to support its high growth rate, rapidly became carbon limited, and the system subsequently flipped to the bleached state (Fig. 4g, h).

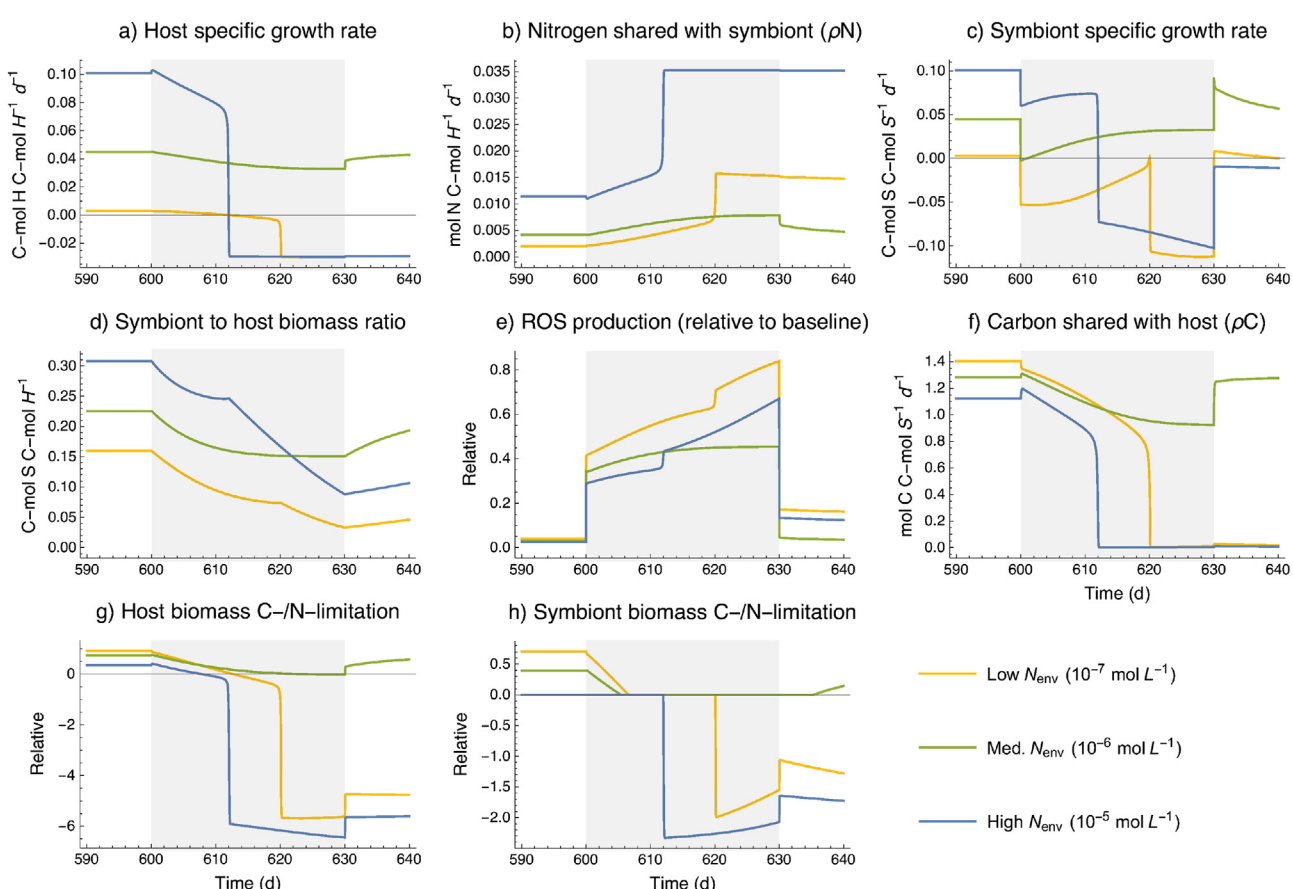
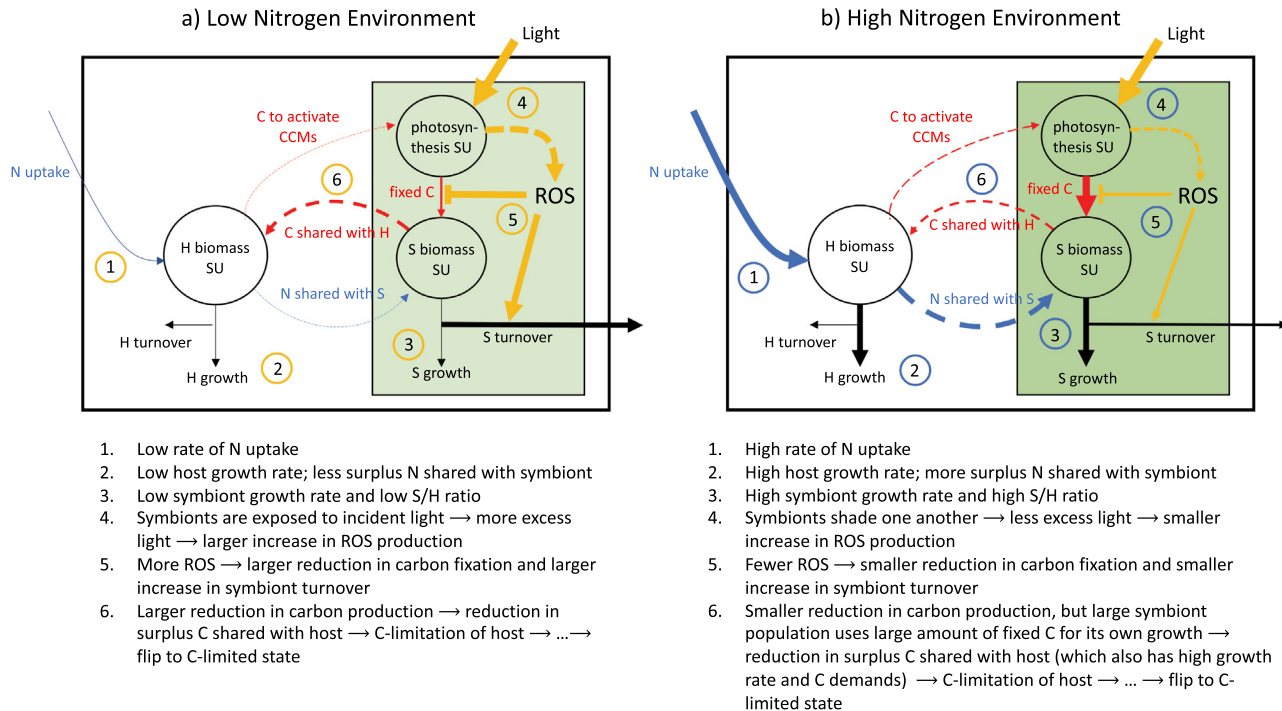


**Fig. 4.** Model simulations of environments with low ( $10^{-7} \text{ mol L}^{-1}$ ), medium ( $10^{-6} \text{ mol L}^{-1}$ ) and high ( $10^{-5} \text{ mol L}^{-1}$ ) values of  $N_{env}$  (the concentration of nitrogen in the external environment) are shown in orange, green, and blue, respectively. All simulations were run without fish or prey, and with a flushing rate of  $d = 1660 \text{ d}^{-1}$ . A light pulse with a total magnitude of  $40 \text{ mol photons m}^{-2} \text{ d}^{-1}$  began at day 600 and lasted 30 days (gray shaded region). For g) and h), positive values indicate biomass production is more limited by nitrogen, while negative values indicate carbon is more limiting.

Nitrogen levels were “just right” if the balance between the protective benefits of dense symbionts and the costs of reduced carbon sharing by these rapidly growing symbionts was sufficient to prevent the system from becoming carbon limited (Fig. 4, green lines). This range of “just right” nitrogen levels depended on the level of stress, and if stress was high enough, it did not exist (the host bleached regardless of nitrogen availability; Fig. S4). Similarly, prey availability also had a large effect on these Goldilocks dynamics; notably, if prey was sufficiently high, the “too low” range either did not exist or occurred at unrealistically low levels of nitrogen (Fig. S5). It is also important to note that once a host had bleached, nitrogen always slowed or inhibited the system’s return to the nitrogen-limited state. Thus, even if nitrogen levels were within the “too low” range, increasing nitrogen had a negative effect on the host’s bleaching response (Fig. S6). It was only when nitrogen jumped from a value in the “too low” range to one in the “just right” range (in which the host does not bleach at all) that an increase in nitrogen availability benefited hosts under stress.

### 3.3. Fish and environmental conditions affect host bleaching and recovery thresholds

#### 3.3.1. Description of analyses

In our model, bleaching occurs when the system transitions from a nitrogen- to a carbon-limited state (Fig. 4), as in the original Cunning et al. (2017) model. Thus, whether or not stress events cause the host to bleach will depend on the relative availability of nitrogen and carbon in the system. The above results suggested that when hosts are stressed, nitrogen can be harmful if “too low” or “too high”, but beneficial if “just right”. Relative nitrogen availability is affected by fish presence as well as environmental conditions (e.g., ambient nitrogen, flushing rates and prey levels; Fig. 2). Thus, we next explored how these factors influenced thresholds in host responses to varying levels of stress.

We ran simulations in which the system was shocked with a light pulse of varying magnitude and duration. In each simulation, the light pulse began on day 600. Pulse duration ( $t_{High}$ ) ranged from 7–35d, and pulse magnitude ( $I_{High} + I$ ) ranged from 35–50 mol photons  $m^{-2} d^{-1}$ . We categorized the system’s response to each stress event as follows: 1) “Not stressed” (host growth remained positive and neither the host nor symbiont biomass SU became carbon-limited), 2) “Mildly stressed” (host growth went negative during the pulse, but both biomass SUs did not become C-limited), 3) “Bleached and recovered” (the system flipped to the bleached state with negative host growth and C-limited SUs, but returned to positive growth and nitrogen limitation within 100 days following the end of the light pulse), and 4) “Bleached with mortality” (the system flipped to the bleached state and remained in this state for more than 100 days after the end of the light pulse). The recovery cut-off of 100 days was chosen because we assumed that a host that still had a negative growth rate after this long would likely be dead.

We first ran these simulations in a low nitrogen, low flushing rate environment ( $N_{env} = 1 * 10^{-7}$  mol  $L^{-1}$ ,  $d = 1660$   $d^{-1}$ ) with and without fish and prey (with  $X = 1 * 10^{-7}$  C-mol  $L^{-1}$  for the with-prey case). We repeated this with a higher flushing rate ( $d = 3000$   $d^{-1}$ ) and then again with higher ambient nitrogen ( $N_{env} = 1 * 10^{-6}$  mol  $L^{-1}$ ).

#### 3.3.2. Results

Fig. 5a-d show the results of simulations in a low nitrogen, low flushing rate environment. In the absence of prey, fish were beneficial under moderate levels of light stress, as hosts without fish were strongly nitrogen limited and unable to maintain positive growth when carbon production was reduced. At higher light

levels, hosts generally bleached regardless of the presence or absence of fish (Fig. 5a, b). However, fish did slightly alter host bleaching thresholds, and these differences were consistent with the finding that “just right” levels of nitrogen depend on the level of stress experienced by the host (Fig. S4). In these simulations, we observed one case in which the presence of fish prevented the host from bleaching (when pulse magnitude was 39 mol photons  $m^{-2} d^{-1}$  and pulse duration was 25d). Exploring this further, we found that slightly increasing environmental nitrogen and decreasing the flushing rate (such that overall nitrogen availability was higher and fish excretions were lost at a slower rate) expanded the range of stress levels for which fish increased nitrogen into the “just right” ranges and prevented bleaching (Fig. S7). However, in the simulations shown in Fig. 5, there were also several cases in which hosts bleached with but not without fish (e.g., at a pulse magnitude of 50 mol photons  $m^{-2} d^{-1}$  and a pulse duration of 7d). At these levels of stress, fish instead increased nitrogen from the “just right” to the “too high” range. Thus, the effects of fish on host bleaching thresholds depended on nitrogen availability in both the presence and absence of fish as well as the severity of the stress event.

Prey increased the host’s tolerance to stress and, for stress levels that exceeded this tolerance, enabled bleached hosts to recover (Fig. 5c). However, recovery required sufficiently low levels of nitrogen: fish reduced the range of stress levels over which recovery was possible (Fig. 5d), while increasing the flushing rate  $d$  ameliorated these negative effects (Fig. 5e, f). Increasing the ambient concentration of nitrogen in the external environment ( $N_{env}$ ) inhibited recovery, with minimal effects of fish (Fig. 5g, h).

### 3.4. Fish and environmental conditions affect post-bleaching recovery

#### 3.4.1. Description of model analyses

While the above analyses indicated whether or not bleached hosts recovered (i.e., returned to the nitrogen-limited state within 100 days after a stress event), we also looked more closely at how these post-bleaching dynamics were affected by fish presence and environmental conditions. To do this, we ran simulations with a light pulse that was stressful enough to induce bleaching across a range of environmental conditions (duration = 30d, magnitude = 50 mol photons  $m^{-2} d^{-1}$ ). We recorded the time the system took to return to the nitrogen-limited state (positive host growth, no carbon limitation) following the end of the pulse. We repeated this with and without fish for varying levels of prey, flushing rates, and ambient nitrogen concentrations. We also varied the relationship between host biomass and fish carrying capacity to explore the effects of fish abundance in addition to presence/absence.

#### 3.4.2. Results

Consistent with Fig. 5, the time the system took to return to the nitrogen-limited state was dependent on the levels of carbon and nitrogen in the holobiont and its environment. Furthermore, the relationship between relative nitrogen availability and return time was nonlinear, with abrupt increases in return times when nitrogen exceeded threshold values (Fig. 6).

Decreasing prey and increasing ambient nitrogen increased the availability of nitrogen relative to that of carbon, slowing the system’s return to the nitrogen-limited state (Fig. 6a, b). Return times were also longer for lower flushing rates (Fig. 6c), highlighting the large effects of interstitial nitrogen dynamics on the system’s response to stress. When the system bleached and the host and symbiont became carbon limited, interstitial nitrogen concentrations spiked due to an increase in surplus nitrogen in the holobiont, which was ultimately released into the interstitial space as waste from the symbionts (Fig. S8). At lower flushing rates, this spike was larger and more prolonged, and there was therefore more nitrogen in the system during the initial post-stress period.

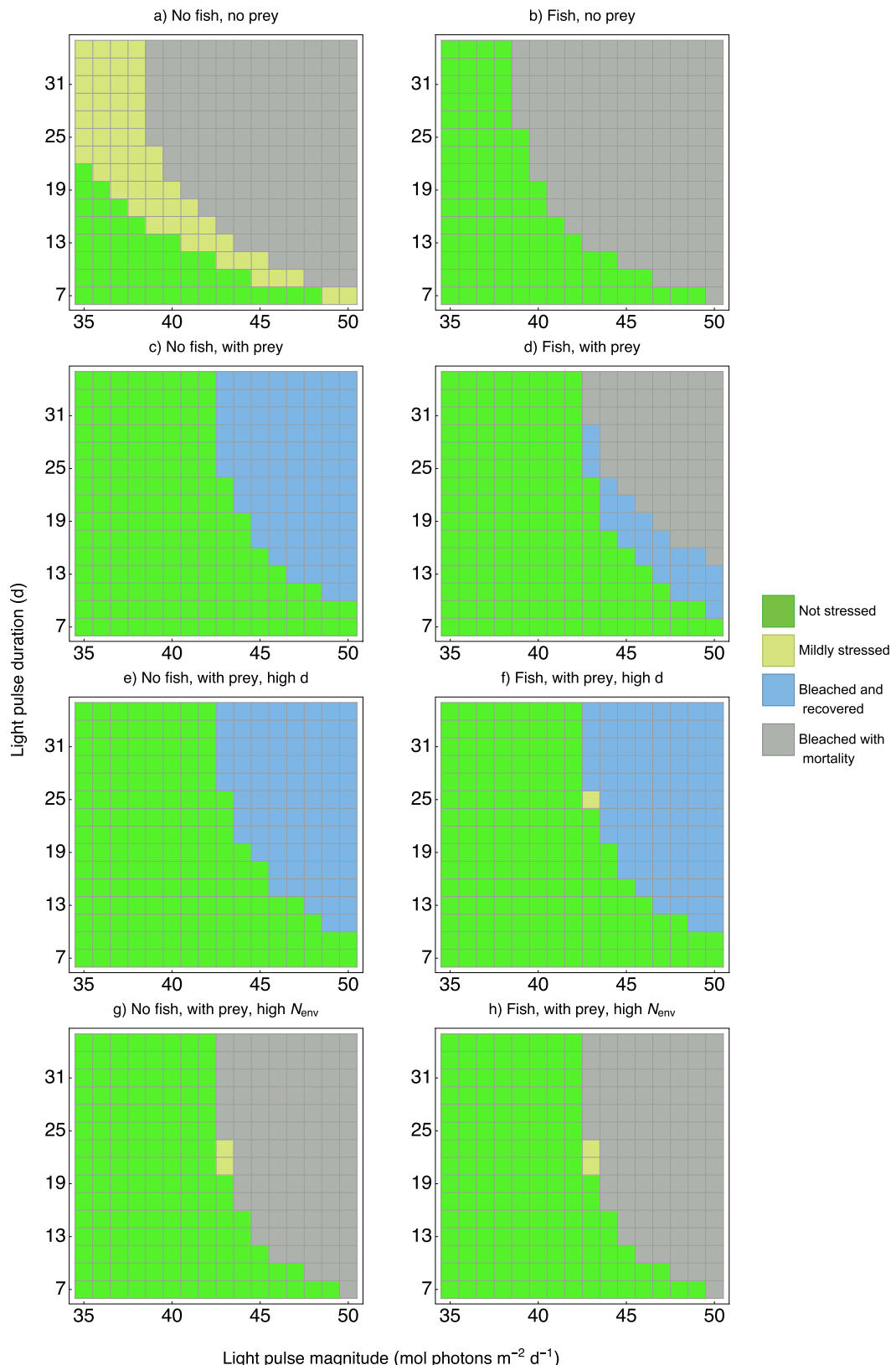


**Fig. 5.** Effects of fish and prey on bleaching thresholds and recovery in different environments. Simulations were run with light pulses of varying magnitudes (x-axis) and durations (y-axis). Pulse magnitude ranged from 35–50 mol photons  $m^{-2} d^{-1}$ , and pulse duration ranged from 7–35 days. For each simulation, the colors indicate whether the host was not stressed, mildly stressed, bleached but recovered, or bleached and died (see “Description of analyses” for the criteria for these categories). For simulations with prey,  $X = 1 \times 10^{-7} \text{ C-mol L}^{-1}$ . a–d)  $N_{env} = 10^{-7} \text{ mol L}^{-1}$  and  $d$  (flushing rate) =  $1660 \text{ d}^{-1}$ . e–f),  $N_{env} = 10^{-7} \text{ mol L}^{-1}$  and  $d = 3000 \text{ d}^{-1}$ , g–h)  $N_{env} = 10^{-6} \text{ mol L}^{-1}$  and  $d = 1660 \text{ d}^{-1}$ .

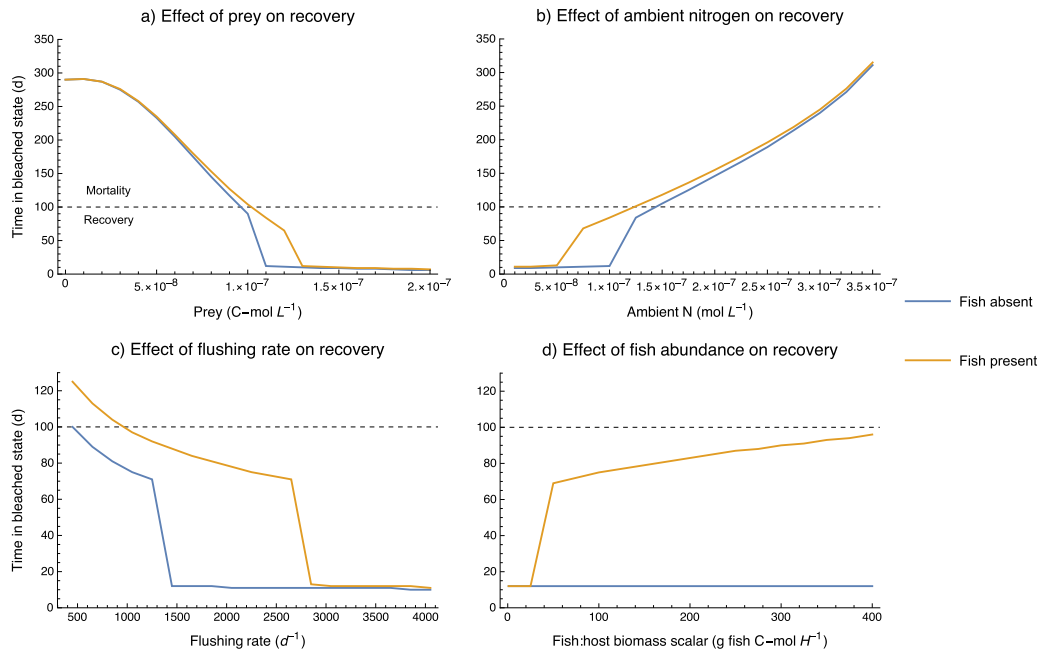


**Fig. 6.** Effects of fish on recovery from bleaching at varying a) levels of prey, b) ambient nitrogen, c) flushing rates, and d) fish abundance. The results of simulations with and without fish are shown in orange and blue, respectively. In all simulations, bleaching was induced with an intense light pulse (magnitude = 50 mol photons  $m^{-2} d^{-1}$ , duration = 30 days) on day 600. The time that it took the system to return to the nitrogen-limited state (i.e., positive host growth, neither partner is C-limited) following the end of the pulse was recorded. In all plots, the dashed horizontal line marks a return time of 100 days. Times less than 100 d correspond to the “Bleached and recovered” scenario in Fig. 5, while longer times correspond to the “Bleached with mortality” scenario. For each plot, the default values for parameters that were held constant were: flushing rate =  $1660 d^{-1}$ , scalar specifying relationship between interstitial host biomass and fish carrying capacity =  $210 g C\text{-mol } H^{-1}$ , ambient N =  $1 \times 10^{-7} mol L^{-1}$ , and prey =  $1.1 \times 10^{-7} C\text{-mol } L^{-1}$ .

Notably, this effect of flushing rate was apparent both with and without fish, despite lower flushing rates reducing the steady state concentration of nitrogen in the interstitial space in the absence of fish (Fig. 2e).

Fish increased the concentration of nitrogen in the interstitial space, resulting in a larger spike in nitrogen levels during bleaching (Fig. S8). This had either neutral or negative effects on host recovery, depending on environmental conditions and fish abundance (Fig. 6). When prey was low and/or ambient nitrogen levels were high, nitrogen availability was well above the system's tipping point, and return times were on the order of several hundred days (note these are not biologically meaningful- the host would likely be dead after this long). Fish declined with host biomass, and the concentration of nitrogen in the interstitial space approached that of the external environment regardless of whether they were initially present (Fig. S9). Fish also had minimal effects on return times when relative nitrogen availability was very low (e.g., when prey was high, environmental nitrogen levels were low, or flushing rate was high). In these cases, nitrogen levels in the presence of fish were still below the threshold value at which an abrupt increase in return time occurred, and the system quickly recovered with or without fish. However, if conditions were such that fish caused nitrogen levels to exceed the system's tipping point, they could greatly increase return times (Fig. 6, Fig. S10). The magnitude of these fish effects was also sensitive to assumptions about fish behavior: if fish carrying capacity scaled to interstitial volume rather than interstitial biomass (i.e., fish did not leave bleached hosts), there were larger increases in return times in their presence (Fig. S11).

#### 4. Discussion

As mass bleaching events threaten coral reef ecosystems around the world (Hughes et al., 2018), it is critically important to understand the factors- both abiotic and biotic- that mediate coral

bleaching. Here, we modified a published DEB model of the coral-algal symbiosis to include the excretions of coral-dwelling fish as a source of nitrogen for host corals. Our model predicted that fish presence can accelerate coral growth rates, but also potentially make host corals more prone to bleaching. The magnitude of fish effects depended on the degree to which they increased nitrogen availability, which was influenced by numerous factors (e.g., ambient nitrogen concentrations, the rate of exchange between the interstitial space and external environment, availability of prey for the host). In low-stress (light) environments, growth was generally nitrogen limited and higher levels of nitrogen were always beneficial. However, during periods of light stress, nitrogen was found to be a “double-edged sword”, potentially increasing a host's tolerance of stress (when not too low or high) but also exacerbating bleaching once the system had entered the carbon-limited state. Thus, while there were certain conditions under which fish could reduce host bleaching susceptibility, when hosts did bleach the presence of fish hindered recovery. Model dynamics under stress were also highly non-linear, and the magnitudes of fish effects on bleaching thresholds and post-bleaching dynamics were sensitive to the degree to which fish altered the relative availability of nitrogen and carbon (i.e., whether fish excretions pushed the system past its tipping points).

In the absence of light stress, fish produced the largest benefits when ambient nitrogen, prey, and flushing rates were low, and when fish biomass per host colony was high (Fig. 2). These results make intuitive sense and are supported by empirical work: in environments where nitrogen is limiting and conditions are such that the interstitial space is not rapidly flushed out, the nitrogen excreted by coral-dwelling fish can enhance the growth of host corals (Holbrook et al., 2008). Coral reefs, particularly those on remote islands less impacted by anthropogenic activities, are generally oligotrophic (Szmant, 2002), and the positive effects of fish excretions may therefore play a significant role in the functioning

of these ecosystems (Allgeier et al., 2016). However, for fish that shelter within individual corals, the degree to which their excretions increase nitrogen availability is influenced by colony flushing rate (Fig. 2e). The flushing rate can be affected by both the flow regime and colony morphology (Reidenbach et al., 2006). Thus, host colonies in low flow environments (e.g., some lagoons; Lowe et al., 2010) would be expected to better retain and utilize fish excretions, as would colonies with more closed branching morphologies (Holbrook et al., 2008). Studies suggest that coral-dwelling fish prefer to shelter in colonies with open morphologies (Chase et al., 2014), leading to a potential trade-off between attracting fish and retaining their excretions (Holbrook et al., 2008). This is predicted by our model, whereby increasing flushing rate (colony openness) and decreasing fish carrying capacity have opposing effects on host growth (Fig. S2b).

When corals were exposed to increased light (a proxy for any stressor that may induce bleaching; e.g., elevated temperature), the effects of fish were more complex. While we found some cases in which fish increased host bleaching tolerance (Fig. 5, Fig. S7), our model also predicted that the presence of fish could put corals at a greater risk of bleaching and mortality. These harmful effects occurred because fish excretions increased the availability of nitrogen relative to that of carbon, which not only made the holobiont more likely to tip into the carbon-limited state when carbon production was disrupted, but also caused it to remain in this state for longer periods of time. Our model predicts that such scenarios are more likely when prey availability is low, flushing rates are low, and ambient nitrogen is high (Fig. 6). Such conditions may occur in lagoon systems, particularly those subject to nitrogen pulses from agricultural or wastewater runoff (Fabricius, 2005); thus, corals in these environments may be more prone to fish-exacerbated bleaching. Especially as bleaching events become more frequent and intense, future field studies could seek to quantify populations of coral-dwelling fishes and link presence and abundance to coral bleaching and recovery in a variety of abiotic settings (Chase et al., 2014 provides one example of such a study, although it is focused on coral growth rather than bleaching). Such data would provide invaluable tests of our model.

Although few empirical studies have explicitly tested the effects of fish presence on host bleaching, recent work suggests fish can reduce bleaching severity and promote post-bleaching recovery (Chase et al., 2018; Pryor et al., 2020). Specifically, experiments with *Pocillopora* corals showed that in the presence of damselfish, corals retained higher symbiont densities and greater photosynthetic capacities during and after a heat shock (Chase et al., 2018). Similar findings have also been reported for photosynthetic anemones hosting anemonefish (Pryor et al., 2020). In part, these empirical results may correspond to regions in model parameter space under which fish excretions provide protective benefits (Fig. S7); however, strictly beneficial effects of fish stand in contrast to our model's predictions. These discrepancies may arise due to differences in physiological responses to light and thermal stress not captured by our model (Tolleter et al., 2013). Additionally, it may be that experimental conditions corresponded to those in which our model predicted minimal effects of fish excretions (e.g., high levels of prey; Fig. 6a). In this case, it may be that other effects of fish underlie their positive effects.

In our model, the only effect of fish presence was to increase interstitial nitrogen levels. In reality, however, coral-dwelling fish can impact their hosts in numerous ways, some of which may be particularly beneficial during periods of stress. For instance, fish movement increases water flow between colony branches, which can reduce hypoxia in the interstitial space and may help to flush out harmful substances that would otherwise accumulate when corals are stressed (Goldshmid et al., 2004; Garcia-Herrera et al., 2017; Nakamura et al., 2005; Chase et al., 2018). It is also possible

that corals, which may feed on particulate organic matter (Palardy et al., 2006), can utilize fish feces as a source of carbon (Bray et al., 1981). Both our results and those of previous studies suggest heterotrophic feeding reduces bleaching severity (Fig. 6a, Cunning et al., 2017; Conti-Jerpe et al., 2020), so this could be another mechanism by which fish benefit corals experiencing photo-oxidative stress. Thus, it is possible that even if fish-derived nitrogen exacerbates host bleaching, this is ameliorated by other positive effects of hosting fish.

Regarding heterotrophic feeding, we made the simplifying assumption that coral prey (which supports heterotrophic growth and nitrogen acquisition by the coral) has the same constant value in the open environment and in the interstitial space. Relatedly, we assumed that this prey is not shared by the coral-dwelling fish (i.e. there is no competition for food between coral and fish; Leray et al., 2019), and that fish are ultimately limited by the volume of interstitial space, not food availability. The assumption of constant prey allowed us to isolate the effects of fish-symbiont feedbacks on coral growth and bleaching, but we note it implies that, unlike nitrogen, the exchange of coral prey between the interstitial space and external environment is rapid enough that coral feeding does not deplete prey in the interstitial space. Although this is undoubtedly a simplification, we confirmed through test computations (not shown) that making interstitial prey dynamic (such that it is affected by exchange with the external environment and uptake by the coral, analogous to nitrogen) has essentially the same effect as reducing constant prey density and thus has no qualitative effects on our results.

When comparing our model predictions to empirical work, it is also necessary to consider the assumptions we made about nutrient dynamics in the coral holobiont. In particular, we assumed all nitrogen (environmental and fish-derived) was of identical chemical form and accessibility. In reality, nitrogen excreted by fishes and other reef animals is mainly in the form of ammonium or urea, while nitrogen in the water column can also include nitrate from natural and anthropogenic (e.g., agricultural runoff) sources (Shantz and Burkepile, 2014). There is growing evidence that nitrate can increase bleaching susceptibility in corals under thermal stress, whereas ammonium may reduce it (Shantz and Burkepile, 2014; Burkepile et al., 2020; Morris et al., 2019; Fernandes de Barros et al., 2020). The mechanisms underlying these differential effects likely involve impacts on photosynthesis and levels of oxidative stress (Morris et al., 2019; Fernandes de Barros et al., 2020). For instance, studies have shown that ammonium enrichment can promote photosynthesis and carbon translocation, while nitrate has the opposite effect (Béraud et al., 2013; Ezzat et al., 2015). Consequently, nitrate enrichment may reduce the stability of the coral-algal symbiosis by shifting it towards symbiont parasitism (Baker et al., 2018; Allgeier et al., 2020). Importantly, the effects of nitrogen enrichment (of any form) on the stress tolerance of the holobiont also depend on phosphorous availability, which is similarly influenced by both fish excretions and anthropogenic activities (Ezzat et al., 2015; Morris et al., 2019). Future iterations of this-and similar-models could therefore account for multiple forms of nitrogen and their associated bioavailabilities and mechanisms of action. In the case of DEB models, this would require additional empirical data quantifying transformation rates between nitrogen forms both within and external to the coral-algal holobiont.

Other model assumptions we made regarding nutrient dynamics related to feedbacks between the holobiont and interstitial nitrogen availability. Specifically, we assumed that waste nitrogen released by the symbiont enters the interstitial space and becomes available to the host. While there is some evidence for such coupling between corals and their symbionts (Tanaka et al., 2018), we note it may be unrealistic for waste nitrogen to enter the inter-

stitial space before it can be utilized (unless it requires processing by interstitial microbes; [Schiller and Herndl, 1989](#); [Rädecker et al., 2015](#)). For the region of parameter space we explored, symbiont waste nitrogen dominated interstitial nitrogen dynamics during periods of stress (Fig. S8e, f), and model predictions were therefore sensitive to its bioavailability (Fig. S12). These results highlight the need for further research on nitrogen cycling within the holobiont ([Rädecker et al., 2015](#)) and, in the context of coral-algal DEB models, for greater consideration of the holobiont's effects on its immediate environment ([Cunning et al., 2017](#); [Muller et al., 2009](#)).

## 5. Conclusion

Corals may benefit from mutualistic interactions with a diverse range of species, and these relationships play a fundamental role in the ability of coral reefs to tolerate and recover from natural and anthropogenic stressors ([Gates and Ainsworth, 2011](#)). However, mutualisms can be context-dependent ([Chamberlain et al., 2014](#)), as illustrated by the breakdown of the coral-algal symbiosis and consequential bleaching of corals ([Lesser, 2011](#)). Our results suggest that the effects of sheltering fish on host corals—specifically those mediated by nutrient excretion—can shift from beneficial to harmful when corals are exposed to high levels of light stress. The contrast between these predictions and the results of empirical studies highlights the need for future work that explores key model assumptions about nutrient dynamics as well as other potential mechanisms by which coral-dwelling fishes may mediate the stress response of their hosts. Ultimately, such work should improve our understanding of how interactions between corals and closely associated fauna influence the capacity for these corals to tolerate the range of stressors they experience.

## Data Availability

All code used in this study can be found at <https://github.com/raine-detmer/Fish-Excretion-Model>.

## Funding

This study was supported by the National Science Foundation (Graduate Research Fellowship to A.R.D., and award EF-1921356 to H.V.M and R.M.N., EF-1921425 to R.C., OCE-1851510 to A.C.S.) and a Simons Foundation Early Career Award in Marine Microbial Ecology and Evolution to H.V.M.

## CRediT authorship contribution statement

**A. Raine Detmer:** Conceptualization, Methodology, Software, Formal analysis, Writing – original draft, Writing – review & editing. **Ross Cunning:** Conceptualization, Methodology, Writing – review & editing. **Ferdinand Pfab:** Methodology, Software, Writing – review & editing. **Alexandra L. Brown:** Methodology, Software, Writing – review & editing. **Adrian C. Stier:** Conceptualization, Writing – review & editing. **Roger M. Nisbet:** Conceptualization, Methodology, Software, Writing – review & editing. **Holly V. Moeller:** Conceptualization, Methodology, Writing – review & editing.

## Declaration of Competing Interest

The authors declare that they have no known competing financial interests or personal relationships that could have appeared to influence the work reported in this paper.

## Acknowledgements

We thank Sally Holbrook, Deron Burkepile, and Peter Edmunds for providing data on fish abundance, fish excretion rates, and coral morphological relationships, respectively. We thank Hollie Putnam, Ariana Huffmyer, and other members of the E5 Coral research team for providing data on coral physiological traits. We also thank S. Holbrook and D. Burkepile for helpful empirical discussions on fish-coral interactions and Ethan Baxter for discussions on model analyses and manuscript drafts.

## Appendix A

Here we provide details on the original [Cunning et al. \(2017\)](#) DEB model of the coral-algal symbiosis. In this model, host and symbiont biomass are both state variables. The flows of nitrogen, carbon and light energy within the system, as well as the formation and turnover of host and symbiont biomass, are described by 14 mass-specific (per unit host or symbiont biomass) fluxes. Biomass formation and the production of fixed carbon by photosynthesis are each described by a parallel complementary synthesizing unit ([Kooijman, 2009](#)) of the general form:

$$F(m; x, y) = \frac{1}{\frac{1}{m} + \frac{1}{x} + \frac{1}{y} - \frac{1}{x+y}}$$

where  $F(m; x, y)$  is the production flux (e.g., rate of biomass formation),  $x$  and  $y$  are the input fluxes of the two substrates used to make the product, and  $m$  is the maximum production rate.

### A.1. Host and symbiont biomass

The changes in host and symbiont biomass are described by ordinary differential equations. For host biomass  $H$ , the mass-specific change in biomass is the difference between the rate of biomass formation  $j_{HG}$  and the rate of biomass turnover  $j_{HT}$  (see [Table 1](#) and [2](#) in the main text for descriptions of model fluxes, parameters, and their units)

$$\frac{dH}{Hdt} = j_{HG} - j_{HT} \quad (\text{A.1})$$

The mass-specific change in symbiont biomass  $S$  is the difference between the rates of biomass formation  $j_{SG}$  and turnover  $j_{ST}$

$$\frac{dS}{Sdt} = j_{SG} - j_{ST} \quad (\text{A.2})$$

The rates of biomass formation and turnover of each partner are functions of the remaining model fluxes, as described in the following sections.

### A.2. Host coral fluxes

Host biomass is produced from nitrogen and organic carbon, which the host receives from several sources. The host takes up dissolved inorganic nitrogen and prey from the environment according to Michaelis–Menten kinetics. The rate of nitrogen uptake  $j_N$  therefore depends on the concentration of nitrogen in the environment  $N$ , the maximum uptake rate  $j_{Nm}$ , and the half-saturation constant  $K_N$ :

$$j_N = \frac{j_{Nm}N}{N + K_N} \quad (\text{A.3})$$

As described in the main text, we modified this equation to distinguish between uptake from the external environment and interstitial space (see eqn. 4 in main text).

Similarly, the rate of prey assimilation  $j_x$  is given by

$$j_X = \frac{j_{Xm}X}{X + K_X} \quad (\text{A.4})$$

where  $X$  is the concentration of prey in the environment (assumed to be constant),  $j_{Xm}$  is the maximum uptake rate, and  $K_X$  is the half-saturation constant (note that in our model, we assumed there was no difference in the feeding rate of tissue in the interstitial space). Prey contains both carbon and nitrogen; the nitrogen obtained from prey is  $n_{NX}j_X$ , where  $n_{NX}$  is the N:C molar ratio of the prey.

In addition to these external sources, the host also acquires nitrogen from the turnover of its own biomass. Turnover  $j_{HT}$  occurs at a constant maintenance rate  $j_{HT}^0$

$$j_{HT} = j_{HT}^0 \quad (\text{A.5})$$

The amount of nitrogen produced by this turnover depends on the N:C molar ratio of host biomass,  $n_{NH}$ . Assuming a proportion  $\sigma_{NH}$  of this nitrogen is recycled, the flux of recycled nitrogen  $r_{NH}$  is therefore given by

$$r_{NH} = \sigma_{NH}n_{NH}j_{HT} \quad (\text{A.6})$$

Finally, the host obtains carbon from the symbiont at a rate dependent on the rejection flux of carbon from the symbiont biomass SU  $\rho_C$  (see eqn. A.22). This rate is per unit symbiont biomass, so it is multiplied by S/H to convert it to per unit host biomass. Putting all of the above together, the rate of host biomass formation  $j_{HG}$  is given by the following synthesizing unit:

$$\begin{aligned} j_{HG} &= F(m; x, y) \\ &= F\left(j_{HGm}; y_C \left( \rho_C \frac{S}{H} + j_X \right), (j_N + n_{NX}j_X + r_{NH})n_{NH}^{-1} \right) \end{aligned} \quad (\text{A.7})$$

where  $m = j_{HGm}$  is the maximum rate of host biomass formation and  $x$  and  $y$  are the input fluxes of carbon and nitrogen, respectively. The parameter  $y_C$  is included to specify the amount of biomass that can be produced from organic carbon.

Parallel synthesizing units are not completely efficient. Even when production is below its maximum rate, not all of the substrates in the input fluxes are able to be used and are instead rejected. The rejection flux of each substrate is equal to the difference between its input flux (the rate at which it enters the SU) and the rate at which it gets incorporated into the SU's product. For the host biomass SU, nitrogen that is in excess of that used for biomass formation makes up a rejection flux  $\rho_N$ :

$$\rho_N = (j_N + n_{NX}j_X + r_{NH} - n_{NH}j_{HG})_+ \quad (\text{A.8})$$

This nitrogen is then available to the symbiont. Note that  $(x)_+$  means  $\max(x, 0)$ , which ensures that the rejection flux is always positive.

The rejection flux of carbon from the host biomass SU,  $j_{eC}$ , is given by

$$j_{eC} = \left( j_X + \rho_C \frac{S}{H} - j_{HG}y_C^{-1} \right)_+ \quad (\text{A.9})$$

This excess carbon is assumed to provide energy for host carbon concentrating mechanisms (CCMs), which concentrate  $\text{CO}_2$  for symbiont photosynthesis.  $j_{CO_2}$ , the flux of  $\text{CO}_2$  that is supplied to the symbiont photosynthesis SU via the host CCMs, is

$$j_{CO_2} = k_{CO_2}j_{eC} \quad (\text{A.10})$$

where that parameter  $k_{CO_2}$  controls how efficient the CCMs are at supplying  $\text{CO}_2$ .

### A.3. Symbiont fluxes

Like the host, symbiont biomass is produced from nitrogen and organic carbon. Organic carbon is produced from light and  $\text{CO}_2$  by a

photosynthesis SU. The rate at which light is absorbed,  $j_L$ , depends on the external irradiance  $I$ , the effective light absorbing cross section of the symbiont  $\bar{a}^*$ , and an amplification factor  $A$ :

$$j_L = AI\bar{a}^* \quad (\text{A.11})$$

The amplification factor describes how internal irradiance (the light available for symbionts to absorb) is modified relative to the external downwelling irradiance by scattering by the coral skeleton as well as by self-shading of the symbionts. It is therefore a function of symbiont density:

$$A = 1.26 + 1.39e^{-6.48\frac{S}{H}} \quad (\text{A.12})$$

$\text{CO}_2$  is actively supplied by the host CCMs ( $j_{CO_2}$ ). In addition, the  $\text{CO}_2$  produced by the formation and turnover of host and symbiont biomass can also be used by the photosynthesis SU. For both the host and symbiont, the flux of recycled  $\text{CO}_2$  ( $r_{CH}$  and  $r_{CS}$  for the host and symbiont, respectively) is equal to the sum of the rate of biomass turnover and the flux of  $\text{CO}_2$  from biomass formation, all multiplied by proportion  $\sigma_C$  of this  $\text{CO}_2$  that is recycled:

$$r_{CH} = \sigma_{CH}(j_{HT} + (1 - y_C)j_{HG}y_C^{-1}) \quad (\text{A.13})$$

$$r_{CS} = \sigma_{CS}(j_{ST}^0 + (1 - y_C)j_{HG}y_C^{-1}) \quad (\text{A.14})$$

From these inputs, the rate of photosynthesis is given by the photosynthesis SU:

$$j_{CP} = F(m; x, y) = F\left(j_{CPm}; y_{CL}j_L, \left(j_{CO_2} + r_{CH}\right)\frac{H}{S} + r_{CS}\right)c_{ROS}^{-1} \quad (\text{A.15})$$

where  $m = j_{CPm}$  is the maximum rate of photosynthesis and  $x$  and  $y$  are the input fluxes of light and  $\text{CO}_2$ , respectively. The flux  $c_{ROS}$ , the relative rate of ROS production (eqn. A.18), results in photoinhibition at high levels of light stress (see below). The rejection flux of light from the photosynthesizing unit,  $j_{eL}$ , is given by

$$j_{eL} = (j_L - j_{CP}y_{CL}^{-1})_+ \quad (\text{A.16})$$

The symbiont is able to quench some of this excess light energy and thus prevent it from damaging the photosystems. Nonphotochemical quenching  $j_{NPQ}$  is described by a single substrate SU, where the substrate is excess light and the maximum NPQ capacity is  $k_{NPQ}$

$$j_{NPQ} = \left( k_{NPQ}^{-1} + j_{eL}^{-1} \right)^{-1} \quad (\text{A.17})$$

Any excess light energy that is not quenched drives the production of reactive oxygen species (ROS). The relative production of ROS ( $c_{ROS}$ ) therefore depends on the rejection flux from the above SU:

$$c_{ROS} = 1 + \frac{(j_{eL} - j_{NPQ})_+}{k_{ROS}} \quad (\text{A.18})$$

where the parameter  $k_{ROS}$  is the amount of excess light energy that doubles ROS production relative to baseline levels. ROS inhibit photosynthesis (eqn. A.15) and also increase the rate of symbiont biomass turnover (due to photodamage and/or expulsion by the host). Therefore, the rate of symbiont biomass turnover  $j_{ST}$  depends not only on the constant maintenance rate  $j_{ST}^0$ , but also on  $c_{ROS}$ , as specified by the scaling parameter  $b$ :

$$j_{ST} = j_{ST}^0(1 + b(c_{ROS} - 1)) \quad (\text{A.19})$$

In addition to the organic carbon produced by photosynthesis, the formation of symbiont biomass also requires nitrogen. The symbiont receives surplus nitrogen from the host ( $\rho_N$ ; eqn. A.8) as well as nitrogen that is recycled from maintenance turnover of symbiont biomass. This flux of recycled nitrogen,  $r_{NS}$ , is the product

of the rate of maintenance symbiont turnover  $j_{ST}^0$ , the N:C molar ratio of symbiont biomass  $n_{NS}$ , and the proportion  $\sigma_{NH}$  of this nitrogen that is recycled:

$$r_{NS} = \sigma_{NS} n_{NS} j_{ST}^0 \quad (\text{A.20})$$

The rate of symbiont biomass formation  $j_{HG}$  is then given by the following synthesizing unit:

$$j_{SG} = F(m; x, y) = F\left(j_{SGm}; y_C j_{CP}, \left(\rho_N \frac{H}{S} + r_{NS}\right) n_{NS}^{-1}\right) \quad (\text{A.21})$$

where  $m = j_{SGm}$  is the maximum rate of host biomass formation and  $x$  and  $y$  are the input fluxes of carbon and nitrogen, respectively.

The surplus carbon that is shared with the host ( $\rho_C$ ) is given by the rejection flux of carbon from this synthesizing unit:

$$\rho_C = j_{CP} - j_{SG} y_C^{-1} \quad (\text{A.22})$$

The rejection flux of nitrogen from the symbiont biomass SU,  $j_{NW}$ , was not explicitly defined in the original model (as it was assumed to be lost to the environment) but is described in eqn. 6 in the main text.

## Appendix B. Supplementary data

Supplementary data associated with this article can be found, in the online version, at <https://doi.org/10.1016/j.jtbi.2022.111087>.

## References

Allgeier, J.E., Andskog, M.A., Hensel, E., Appaldo, R., Layman, C., Kemp, D.W., 2020. Rewiring coral: Anthropogenic nutrients shift diverse coral-symbiont nutrient and carbon interactions toward symbiotic algal dominance. *Glob. Change Biol.* 26 (10), 5588–5601.

Allgeier, J.E., Valdivia, A., Cox, C., Layman, C.A., 2016. Fishing down nutrients on coral reefs. *Nat. Commun.* 7 (1), 12461.

Baker, D.M., Freeman, C.J., Wong, J.C., Fogel, M.L., Knowlton, N., 2018. Climate change promotes parasitism in a coral symbiosis. *ISME J.* 12 (3), 921–930.

Booth, D.J., 2016. Ability to home in small site-attached coral reef fishes: homing in site-attached coral reef fishes. *J. Fish Biol.* 89 (2), 1501–1506.

Bray, R.N., Miller, A.C., Geesey, G.G., 1981. The Fish Connection: A Trophic Link Between Planktonic and Rocky Reef Communities? *Science* 214 (4517), 204–205.

Burkepile, D.E., Shantz, A.A., Adam, T.C., Munsterman, K.S., Speare, K.E., Ladd, M.C., Rice, M.M., Ezzat, L., McIlroy, S., Wong, J.C.Y., Baker, D.M., Brooks, A.J., Schmitt, R.J., Holbrook, S.J., 2020. Nitrogen Identity Drives Differential Impacts of Nutrients on Coral Bleaching and Mortality. *Ecosystems* 23 (4), 798–811.

Béraud, E., Gevaert, F., Rottier, C., Ferrier-Pagès, C., 2013. The response of the scleractinian coral *Turbinaria reniformis* to thermal stress depends on the nitrogen status of the coral holobiont. *J. Exp. Biol.* 216 (14), 2665–2674.

Chamberlain, J., Graus, R., 1975. Water Flow and Hydromechanical Adaptations of Branched Reef Corals. *Bull. Mar. Sci.* 25, 112–215.

Chamberlain, S.A., Bronstein, J.L., Rudgers, J.A., 2014. How context dependent are species interactions? *Ecol. Lett.* 17 (7), 881–890.

Chase, T.J., Pratchett, M.S., Frank, G.E., Hoogenboom, M.O., 2018. Coral-dwelling fish moderate bleaching susceptibility of coral hosts. *PLOS ONE* 13, (12) e0208545.

Chase, T.J., Pratchett, M.S., Walker, S.P.W., Hoogenboom, M.O., 2014. Small-scale environmental variation influences whether coral-dwelling fish promote or impede coral growth. *Oecologia* 176 (4), 1009–1022.

Clark, C.D., Mumby, P.J., Chisholm, J.R.M., Jaubert, J., Andrefouet, S., 2000. Spectral discrimination of coral mortality states following a severe bleaching event. *Int. J. Remote Sens.* 21 (11), 2321–2327.

Coker, D.J., Pratchett, M.S., Munday, P.L., 2012. Influence of coral bleaching, coral mortality and conspecific aggression on movement and distribution of coral-dwelling fish. *J. Exp. Mar. Biol. Ecol.* 414–415, 62–68.

Coker, D.J., Wilson, S.K., Pratchett, M.S., 2014. Importance of live coral habitat for reef fishes. *Rev. Fish Biol. Fisheries* 24 (1), 89–126.

Conti-Jerpe, I.E., Thompson, P.D., Wong, C.W.M., Oliveira, N.L., Duprey, N.N., Moynihan, M.A., Baker, D.M., 2020. Trophic strategy and bleaching resistance in reef-building corals. *Sci. Adv.* 6 (15). eaaz5443.

Crossland, C.J., Hatcher, B.G., Smith, S.V., 1991. Role of coral reefs in global ocean production. *Coral Reefs* 10 (2), 55–64.

Cruz-Pinon, G., Carricart-Ganivet, J.P., Espinoza-Avalos, J., 2003. Monthly skeletal extension rates of the hermatypic corals *Montastraea annularis* and *Montastraea faveolata*: biological and environmental controls. *Mar. Biol.* 143 (3), 491–500.

Cunning, R., Muller, E.B., Gates, R.D., Nisbet, R.M., 2017. A dynamic bioenergetic model for coral-*Symbiodinium* symbioses and coral bleaching as an alternate stable state. *J. Theor. Biol.* 431, 49–62.

Davy, S.K., Allemand, D., Weis, V.M., 2012. Cell Biology of Cnidarian-Dinoflagellate Symbiosis. *Microbiol. Mol. Biol. Rev.* 76 (2), 229–261.

Donovan, M.K., Adam, T.C., Shantz, A.A., Speare, K.E., Munsterman, K.S., Rice, M.M., Schmitt, R.J., Holbrook, S.J., Burkepile, D.E., 2020. Nitrogen pollution interacts with heat stress to increase coral bleaching across the seascape. *Proc. Nat. Acad. Sci.* 117 (10), 5351–5357.

Eakin, C.M., Sweatman, H.P.A., Brainard, R.E., 2019. The 2014–2017 global-scale coral bleaching event: insights and impacts. *Coral Reefs* 38 (4), 539–545.

Ezzat, L., Maguer, J.-F., Grover, R., Ferrier-Pagès, C., 2015. New insights into carbon acquisition and exchanges within the coral-dinoflagellate symbiosis under  $[\text{NH}_4^+]$  and  $[\text{NO}_3^-]$  supply. *Proc. R. Soc. B: Biol. Sci.* 282 (1812), 20150610.

Fabricius, K.E., 2005. Effects of terrestrial runoff on the ecology of corals and coral reefs: review and synthesis. *Mar. Pollut. Bull.* 50 (2), 125–146.

de Barros, Fernandes, Marangoni, L., Ferrier-Pagès, C., Rottier, C., Bianchini, A., Grover, R., 2020. Unravelling the different causes of nitrate and ammonium effects on coral bleaching. *Scientific Rep.* 10 (1), 11975.

Fisher, R., O'Leary, R., Low-Choy, S., Mengersen, K., Knowlton, N., Brainard, R., Caley, M., 2015. Species Richness on Coral Reefs and the Pursuit of Convergent Global Estimates. *Curr. Biol.* 25 (4), 500–505.

Fox, M.D., Williams, G.J., Johnson, M.D., Radice, V.Z., Zgliczynski, B.J., Kelly, E.L., Rohwer, F.L., Sandin, S.A., Smith, J.E., 2018. Gradients in Primary Production Predict Trophic Strategies of Mixotrophic Corals across Spatial Scales. *Curr. Biol.* 28 (21), 3355–3363.e4.

Garcia-Herrera, N., Ferse, S.C.A., Kunzmann, A., Genin, A., 2017. Mutualistic damselfish induce higher photosynthetic rates in their host coral. *J. Exp. Biol.* 220 (10), 1803–1811.

Gates, R.D., Ainsworth, T.D., 2011. The nature and taxonomic composition of coral symbioses as drivers of performance limits in scleractinian corals. *J. Exp. Mar. Biol. Ecol.* 408 (1–2), 94–101.

Gil, M.A., 2013. Unity through nonlinearity: a unimodal coral-nutrient interaction. *Ecology* 94 (8), 1871–1877.

Goldshmid, R., Holzman, R., Weih, D., Genin, A., 2004. Aeration of corals by sleep-swimming fish. *Limnol. Oceanogr.* 49 (5), 1832–1839.

Graham, N.A.J., Nash, K.L., 2013. The importance of structural complexity in coral reef ecosystems. *Coral Reefs* 32, 315–326.

Grottoli, A.G., Rodrigues, L.J., Palaridy, J.E., 2006. Heterotrophic plasticity and resilience in bleached corals. *Nature* 440 (7088), 1186–1189.

Hackerott, S., Martell, H.A., Eirin-Lopez, J.M., 2021. Coral environmental memory: causes, mechanisms, and consequences for future reefs. *Trends Ecol. Evol.* 36 (11), 1011–1023.

Henry, L.-A., Hart, M., 2005. Regeneration from Injury and Resource Allocation in Sponges and Corals - a Review. *Int. Rev. Hydrobiol.* 90 (2), 125–158.

Hoegh-Guldberg, O., 1999. Climate change, coral bleaching and the future of the world's coral reefs. *Mar. Freshwater Res.* 50 (8), 839–866.

Holbrook, S.J., Brooks, A.J., Schmitt, R.J., Stewart, H.L., 2008. Effects of sheltering fish on growth of their host corals. *Mar. Biol.* 155 (5), 521–530.

Holbrook, S.J., Schmitt, R.J., 2002. Competition for shelter space causes density-dependent predation mortality in damselfishes. *Ecology* 83 (10), 2855–2868.

Hughes, T.P., Anderson, K.D., Connolly, S.R., Heron, S.F., Kerry, J.T., Lough, J.M., Baird, A.H., Baum, J.K., Berumen, M.L., Bridge, T.C., Claar, D.C., Eakin, C.M., Gilmour, J.P., Graham, N.A.J., Harrison, H., Hobbs, J.-P.A., Hoey, A.S., Hoogenboom, M., Lowe, R.J., McCulloch, M.T., Pandolfi, J.M., Pratchett, M., Schoepf, V., Torda, G., Wilson, S.K., 2018. Spatial and temporal patterns of mass bleaching of corals in the Anthropocene. *Science* 359 (6371), 80–83.

Jones, G.P., 1986. Food availability affects growth in a coral reef fish. *Oecologia* 70 (1), 136–139.

Kane, C.N., Brooks, A.J., Holbrook, S.J., Schmitt, R.J., 2009. The role of microhabitat preference and social organization in determining the spatial distribution of a coral reef fish. *Environ. Biol. Fishes* 84 (1), 1–10.

Kooijman, B., 2009. Dynamic Energy Budget Theory for Metabolic Organisation. Cambridge University Press, Cambridge, third ed..

Leray, M., Alldredge, A.L., Yang, J.Y., Meyer, C.P., Holbrook, S.J., Schmitt, R.J., Knowlton, N., Brooks, A.J., 2019. Dietary partitioning promotes the coexistence of planktivorous species on coral reefs. *Mol. Ecol.* 28 (10), 2694–2710.

Lesser, M.P., 2011. Coral Bleaching: Causes and Mechanisms. In: Dubinsky, Z., Stambler, N. (Eds.), *Coral Reefs: An Ecosystem in Transition*. Springer, Netherlands, Dordrecht, pp. 405–419.

Liberman, T., Genin, A., Loya, Y., 1995. Effects on growth and reproduction of the coral *Stylophora pistillata* by the mutualistic damselfish *Dascyllus marginatus*. *Mar. Biol.* 121 (4), 741–746.

Lowe, R.J., Hart, C., Pattiaratchi, C.B., 2010. Morphological constraints to wave-driven circulation in coastal reef-lagoon systems: A numerical study. *J. Geophys. Res.* 115 (C9), C09021.

Loya, Y., Sakai, K., Yamazato, K., Nakano, Y., Sambali, H., van Woesik, R., 2001. Coral bleaching: the winners and the losers. *Ecol. Lett.* 4 (2), 122–131.

McKeon, C.S., Stier, A.C., McIlroy, S.E., Bolker, B.M., 2012. Multiple defender effects: synergistic coral defense by mutualist crustaceans. *Oecologia* 169 (4), 1095–1103.

Meyer, J.L., Schultz, E.T., 1985. Migrating haemulid fishes as a source of nutrients and organic matter on coral reefs: N, P, and POC from reef fish. *Limnol. Oceanogr.* 30 (1), 146–156.

Morris, L.A., Voolstra, C.R., Quigley, K.M., Bourne, D.G., Bay, L.K., 2019. Nutrient Availability and Metabolism Affect the Stability of Coral-Symbiodiniaceae Symbioses. *Trends Microbiol.* 27 (8), 678–689.

Muller, E.B., Kooijman, S.A., Edmunds, P.J., Doyle, F.J., Nisbet, R.M., 2009. Dynamic energy budgets in syntrophic symbiotic relationships between heterotrophic hosts and photoautotrophic symbionts. *J. Theor. Biol.* 259 (1), 44–57.

Muscatine, L., Porter, J.W., 1977. Reef Corals: Mutualistic Symbioses Adapted to Nutrient-Poor Environments. *Bioscience* 27 (7), 454–460.

Nakajima, R., Yoshida, T., Othman, B.H.R., Toda, T., 2014. Biomass and estimated production rates of metazoan zooplankton community in a tropical coral reef of Malaysia. *Mar. Ecol.* 35 (1), 112–131.

Nakamura, T., van Woesik, R., Yamasaki, H., 2005. Photoinhibition of photosynthesis is reduced by water flow in the reef-building coral *Acropora digitifera*. *Mar. Ecol. Prog. Ser.* 301, 109–118.

O'Neil, J.M., Capone, D.G., 2008. Nitrogen Cycling in Coral Reef Environments. In: Nitrogen in the Marine Environment. Elsevier, pp. 949–989.

Palardy, J.E., Grottoli, A.G., Matthews, K.A., 2006. Effect of naturally changing zooplankton concentrations on feeding rates of two coral species in the Eastern Pacific. *J. Exp. Mar. Biol. Ecol.* 331 (1), 99–107.

Pfab, F., Brown, A.L., Detmer, A.R., Baxter, E.C., Moeller, H.V., Cunning, R., and Nisbet, R.M. (in review). Time scale separation in models of symbiosis: State space reduction, multiple attractors and initialization. *Conservation Physiology*.

Pinnegar, J.K., Polunin, N.V.C., 2006. Planktivorous damselfish support significant nitrogen and phosphorus fluxes to Mediterranean reefs. *Mar. Biol.* 148 (5), 1089–1099.

Pollock, F.J., Katz, S.M., Bourne, D.G., Willis, B.L., 2013. Cymo melanodactylus crabs slow progression of white syndrome lesions on corals. *Coral Reefs* 32 (1), 43–48.

Pryor, S.H., Hill, R., Dixson, D.L., Fraser, N.J., Kelaher, B.P., Scott, A., 2020. Anemonefish facilitate bleaching recovery in a host sea anemone. *Scientific Rep.* 10 (1), 18586.

Reidenbach, M.A., Koseff, J.R., Monismith, S.G., Steinbuck, J.V., Genin, A., 2006. The effects of waves and morphology on mass transfer within branched reef corals. *Limnol. Oceanogr.* 51 (2), 1134–1141.

Roman, M.R., Furnas, M.J., Mullin, M.M., 1990. Zooplankton abundance and grazing at Davies Reef, Great Barrier Reef, Australia. *Mar. Biol.* 105 (1), 73–82.

Rowan, R., 2004. Thermal adaptation in reef coral symbionts. *Nature* 430 (7001), 742–742.

Rädecker, N., Pogoreutz, C., Voolstra, C.R., Wiedenmann, J., Wild, C., 2015. Nitrogen cycling in corals: the key to understanding holobiont functioning? *Trends Microbiol.* 23 (8), 490–497.

Schiller, C., Herndl, G.J., 1989. Evidence of enhanced microbial activity in the interstitial space of branched corals: possible implications for coral metabolism. *Coral Reefs* 7 (4), 179–184.

Sebens, K.P., Helmuth, B., Carrington, E., Agius, B., 2003. Effects of water flow on growth and energetics of the scleractinian coral *Agaricia tenuifolia* in Belize. *Coral Reefs* 22 (1), 35–47.

Shantz, A.A., Burkepile, D.E., 2014. Context-dependent effects of nutrient loading on the coral-algal mutualism. *Ecology* 95 (7), 1995–2005.

Spalding, M., Ravilious, C., and Green, E.P. (2001). *World atlas of coral reefs*. University of California Press, Berkeley. Num Pages: 1.

Stella, J.S., Jones, G.P., Pratchett, M.S., 2010. Variation in the structure of epifaunal invertebrate assemblages among coral hosts. *Coral Reefs* 29 (4), 957–973.

Stewart, H.L., Holbrook, S.J., Schmitt, R.J., Brooks, A.J., 2006. Symbiotic crabs maintain coral health by clearing sediments. *Coral Reefs* 25 (4), 609–615.

Szmant, A.M., 2002. Nutrient enrichment on coral reefs: Is it a major cause of coral reef decline? *Estuaries* 25 (4), 743–766.

Tanaka, Y., Suzuki, A., Sakai, K., 2018. The stoichiometry of coral-dinoflagellate symbiosis: carbon and nitrogen cycles are balanced in the recycling and double translocation system. *ISME J.* 12 (3), 860–868.

Tolleter, D., Seneca, F., DeNofrio, J., Krediet, C., Palumbi, S., Pringle, J., Grossman, A., 2013. Coral Bleaching Independent of Photosynthetic Activity. *Curr. Biol.* 23 (18), 1782–1786.

Vega Thurber, R.L., Burkepile, D.E., Fuchs, C., Shantz, A.A., McMinds, R., Zaneveld, J.R., 2014. Chronic nutrient enrichment increases prevalence and severity of coral disease and bleaching. *Glob. Change Biol.* 20 (2), 544–554.

Wiedenmann, J., D'Angelo, C., Smith, E.G., Hunt, A.N., Legiret, F.-E., Postle, A.D., Achterberg, E.P., 2013. Nutrient enrichment can increase the susceptibility of reef corals to bleaching. *Nat. Clim. Change* 3 (2), 160–164.

Wilson, S.K., Burgess, S.C., Cheal, A.J., Emslie, M., Fisher, R., Miller, I., Polunin, N.V.C., Sweatman, H.P.A., 2008. Habitat utilization by coral reef fish: implications for specialists vs. generalists in a changing environment. *J. Anim. Ecol.* 77 (2), 220–228.

Wooldridge, S.A., 2009. A new conceptual model for the warm-water breakdown of the coral - algae endosymbiosis. *Mar. Freshwater Res.* 60 (6), 483.